TURUN YLIOPISTON JULKAISUJA
ANNALES UNIVERSITATIS TURKUENSIS

SARJA - SER. D OSA - TOM. 874

MEDICA - ODONTOLOGICA

NON-RESORBABLE GLASS FIBRE-REINFORCED COMPOSITE WITH POROUS SURFACE AS BONE SUBSTITUTE MATERIAL

Experimental studies *in vitro* and *in vivo* focused on bone-implant interface

by

Riina Mattila

TURUN YLIOPISTO
UNIVERSITY OF TURKU
Turku 2009

From the Department of Prosthetic Dentistry and Biomaterials Science, Institute of Dentistry, University of Turku, Turku, Finland

Supervised by Professor Pekka Vallittu
Department of Prosthetic Dentistry and Biomaterials Science
Institute of Dentistry, University of Turku
Turku, Finland.

Professor Allan Aho
Department of Surgery
Orthopaedic Unit
Turku University Central Hospital
Turku, Finland

Reviewed by Professor Reijo Lappalainen
Department of Physics & BioMater Centre
University of Kuopio
Kuopio, Finland

Associate professor Rui L. Reis
3B's Research Group
Department of Polymer Engineering
University of Minho
Guimarães, Portugal

Opponent Professor Jukka Seppälä
Department of Biotechnology and Chemical Technology
Faculty of Chemistry and Materials Science
Helsinki University of Technology
Helsinki, Finland

ISBN 978-951-29-4066-0 (PRINT)
ISBN 978-951-29-4067-7 (PDF)
ISSN 0355-9483
Painosalama Oy – Turku, Finland 2009

Miksi kiirehtiä, kun aikaa kuitenkin tulee koko ajan lisää.

~ Afrikkalainen sananlasku ~

ABSTRACT

Riina Mattila. Non-resorbable glass fibre-reinforced composite with porous surface as bone substitute material: Experimental studies *in vitro* and *in vivo* focused on bone-implant interface. Department of Prosthetic Dentistry and Biomaterials Science, Institute of Dentistry, University of Turku. *Annales Universitatis Turkuensis*, Turku, Finland, 2009.

The development of load-bearing osseous implant with desired mechanical and surface properties in order to promote incorporation with bone and to eliminate risk of bone resorption and implant failure is a very challenging task. Bone formation and resoption processes depend on the mechanical environment. Certain stress/strain conditions are required to promote new bone growth and to prevent bone mass loss. Conventional metallic implants with high stiffness carry most of the load and the surrounding bone becomes virtually unloaded and inactive. Fibre-reinforced composites offer an interesting alternative to metallic implants, because their mechanical properties can be tailored to be equal to those of bone, by the careful selection of matrix polymer, type of fibres, fibre volume fraction, orientation and length. Successful load transfer at bone-implant interface requires proper fixation between the bone and implant. One promising method to promote fixation is to prepare implants with porous surface. Bone ingrowth into porous surface structure stabilises the system and improves clinical success of the implant.

The experimental part of this work was focused on polymethyl methacrylate (PMMA) -based composites with dense load-bearing core and porous surface. Three-dimensionally randomly orientated chopped glass fibres were used to reinforce the composite. A method to fabricate those composites was developed by a solvent treatment technique and some characterisations concerning the functionality of the surface structure were made *in vitro* and *in vivo*. Scanning electron microscope observations revealed that the pore size and interconnective porous architecture of the surface layer of the fibre-reinforced composite (FRC) could be optimal for bone ingrowth. Microhardness measurements showed that the solvent treatment did not have an effect on the mechanical properties of the load-bearing core. A push-out test, using dental stone as a bone model material, revealed that short glass fibre-reinforced porous surface layer is strong enough to carry load. Unreacted monomers can cause the chemical necrosis of the tissue, but the levels of leachable resisidual monomers were considerably lower than those found in chemically cured fibre-reinforced dentures and in modified acrylic bone cements. Animal experiments proved that surface porous FRC implant can enhance fixation between bone and FRC. New bone ingrowth into the pores was detected and strong interlocking between bone and the implant was achieved.

Keywords: Bone substitute material, fibre-reinforced composite, porosity.

TIIVISTELMÄ

Riina Mattila. Pinnaltaan huokoinen resorboitumaton lasikuitulujitettu komposiitti luuta korvaavana materiaalina: Luu-implantti -rajapintaa koskevia kokeellisia *in vitro* ja *in vivo* -tutkimuksia. Hammasprotetiikan ja biomateriaalitieteen oppiaine, Hammaslääketieteen laitos, Turun yliopisto. *Annales Universitatis Turkuensis*, Turku, Finland, 2009.

Mekaanisilta ja pintaominaisuuksiltaan optimaalisen kuormaa kantavan luuta korvaavan implantin kehitystyö, jonka tavoitteena on saavuttaa luun ja implantin välinen kiinnittyminen, on haastava tehtävä. Luun kasvun edistämiseksi ja luun resorption ehkäisemiseksi tarvitaan tietynlaiset jännitys/venymä -olosuhteet. Perinteiset metalliset implantit, joiden jäykkyys on suuri, kantavat suurimman osan kuormasta ja ympärillä oleva luu jää käytännössä alikuormittuneeksi ja inaktiiviseksi. Kuitulujitteiset komposiitit tarjoavat mielenkiintoisen vaihtoehdon metalli-implanteille, sillä niiden mekaanisia ominaisuuksia voidaan räätälöidä luun kanssa samankaltaisiksi valitsemalla järkevästi matriisin muodostavan polymeerin, käytettävät kuitulujitteet sekä niiden määrän, orientaation ja pituuden. Onnistunut kuormansiirto luu-implantti -rajapinnalla vaatii luun ja implantin välisen kiinnittymisen. Eräs lupaava menetelmä on implantin pinnan tekeminen huokoiseksi. Luun kasvu huokosrakenteeseen stabiloi systeemin ja parantaa implantin menestymismahdollisuutta kliinisessä käytössä.

Väitöskirjatyön kokeellinen osuus keskittyi polymetyylimetakrylaatti (PMMA) -pohjaisiin komposiitteihin, joilla on tiivis kuormaakantava ydin ja huokoinen pintakerros. Kolmiulotteisesti sattumanvaraisesti orientoituneita katkolasikuituja käytettiin lujittamaan komposiittia. Tässä väitöskirjatyössä kehitettiin menetelmä näiden komposiittien valmistamiseksi liuotinkäsittelymenetelmän avulla ja tehtiin joitakin pintarakenteen toiminnallisuuteen liittyviä karakterisointeja *in vitro* ja *in vivo*. Elektronimikroskooppitarkastelut osoittivat, että huokoiskoko ja toisiinsa yhteenliittyneiden huokosten verkosto kuitulujitteisen komposiitin (FRC) pintakerroksessa voisi olla optimaalinen luun sisäänkasvulle. Mikrokovuusmittaukset osoittivat, että liuotinkäsittely ei vaikuta komposiitin ytimen mekaanisiin ominaisuuksiin. Push-out –testi, jossa käytettiin kipsiä luuta simuloivana materiaalinen, osoitti, että katkolasikuiduilla vahvistettu huokoinen pintakerros on riittävän vahva kantaakseen kuormaa. Reagoimattoman monomeerien voivat aiheuttaa kudosten kemiallista nekroosia, mutta vapautuvan metyylimetakrylaattimonomeerin (MMA) pitoisuus oli huomattavasti alhaisempi kuin kemiallisesti kovetettavissa hammasproteeseissa ja modifioiduissa akryyliluusementeissä. Eläinkokeet osoittivat, että pinnaltaan huokoinen FRC implantti pystyy edistämään luun ja implantin välistä kiinnittymistä. Luun sisäänkasvua huokosiin havaittiin ja vahva lukkiutuminen luun ja implantin välille saatiin aikaan.

Avainsanat: Luuta korvaava materiaali, kuitulujitettu komposiitti, huokoisuus.

TABLE OF CONTENTS

ABBREVIATIONS

BAG	Bioactive glass
BCI	Bone contact index
E-glass	Electrical grade glass
FEA	Finite element analysis
FRC	Fibre-reinforced composite
GF	Glass fibre
HPLC	High performance liquid chromatography
i.m.	Intramuscular
IPF	Interfacial porosity formation
MMA	Methyl methacrylate
M_w	Weight average molecular weight
PMMA	Polymethyl methacrylate
ppm	Parts per million
PS	Porous surface
R_a	Average roughness
s.c.	Subcutaneous
SED	Strain energy density
S53P4	Bioactive glass with silica content of 53%
SEM	Scanning electron microscopy
SiC	Silicon carbide
THF	Tetrahydrofuran
Ti	Titanium
UV	Ultra violet
VHN	Vickers hardness number
µCT	Microcomputed tomography

DEFINITIONS

Allograft is a graft (e.g. bone graft) taken from another individual of the same species as the recipient (Williams, 1999)

Autograft is a graft taken from the individual who receives it (Williams, 1999).

Bioactive glass is any glass or ceramic that displays the characteristics of bioactivity (Williams, 1999).

Bioactivity is a phenomenon by which a biomaterial elicits or modulates a biological response at the interface of the material that results in the formation of a bond between the tissue and the material (Williams, 1999).

Biocompatibility is an ability of a material used in a medical device to perform with an appropriate host response in a specific application (Williams, 1999).

Biomaterial is a material intended to interact with biological systems to evaluate, treat, augment or replace any tissue, organ of function of a body (Williams, 1999).

Critical size defect can not be expected to heal by new bone formation by nature (Williams, 1999).

Fatigue of the material under cyclic loading occurs at stress levels that are low relative to the yield strength (Callister, 2007)

Finite element analysis is a numerical technique for finding approximate solutions of partial differential equations as well as of integral equations. Finite element analysis consists of a computer model of a material or design that is stressed and analyzed for specific results (Williams, 1999).

Implant is a medical device made from one or more biomaterials intentionally placed within the body, either totally or partially buried beneath an epithelial surface (Williams, 1999).

Isotropic means uniform; properties of the material are independent on the direction (Williams, 1999).

Osseointegration refers to direct structural and functional connection between living bone and the surface of a load-bearing implant (Williams, 1999).

Osteoconductivity is the ability of an implant to guide bone ingrowth (Williams, 1999).

Viscoelastic creep is time-dependent deformation of polymeric materials under constant stress (Callister, 2007).

LIST OF ORIGINAL PUBLICATIONS

This thesis is based on the following original articles, which are referred to in the text by the Roman numerals I-IV. The original publications are reproduced with the permission of the copyright holders.

I **Mattila RH, Lassila LVJ, Vallittu PK.** Production and structural characterisation of porous fibre-reinforced composite. Composites, Part A: Applied Science and Manufacturing 2004;35A(6): 631-636.

II **Mattila RH, Puska MA, Lassila LVJ, Vallittu PK.** Fibre-reinforced composite implant: *in vitro* mechanical interlocking with bone model material and residual monomer analysis. Journal of Materials Science: Materials in Medicine 2006;41(13): 4321-4326.

III **Mattila RH, Laurila P, Rekola J, Gunn J, Lassila LVJ, Mäntylä T, Aho AJ, Vallittu PK.** Bone attachment to glass fibre-reinforced composite implant with porous surface. Acta biomaterialia 2009; 5(5): 1639-1646.

IV **Mattila RH, Rekola J, Gunn J, Lassila LVJ, Svedström E, Aho AJ, Vallittu PK.** Fibre-reinforced composite with porous surface as a bone substitute implant. Histological, histomorphometric and microradiographic analysis of the bone-implant interface: An experimental study in rabbits. Submitted.

1. INTRODUCTION

Composite materials may be defined as those materials that consist of two or more fundamentally different components that are able to act synergistically to give properties superior to those provided by either component alone (Williams, 1999). A simple classification of man-made composite materials is presented in Figure 1.

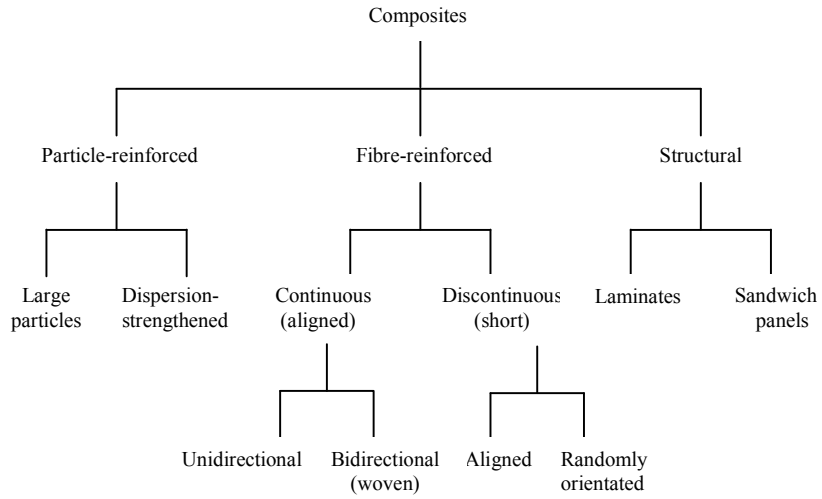

Figure 1. A classification scheme of the various composite types. The figure has been modified from Callister (Callister, 2007).

Bone is a biological composite material in which cells make up only 2-5% of the volume. Mineral-encrusted protein matrix forms 95-98% of bone tissue. All cells are embedded in this matrix and communicate with each other through an extensive network of cellular processes lying in channels, which spread out through the bone. The inorganic part, consisting principally hydroxyapatite, comprises about half the volume of the matrix and gives bone its mechanical properties, such as stiffness, hardness and resiliency. The organic matrix of bone consists predominantly of collagen (mainly type I) and various growth factors. Bone macroscopic structure can be divided into two types: compact cortical bone and spongy trabecular or cancellous bone (Jee, 2001).

Several conditions can cause permanent loss of bone including irreparable damage due trauma, arthritic diseases, musculoskeletal defects, removal of malignant tumours and replacement of failed implants. Metals, such as pure or alloyed forms of titanium, are today the most widely used implant materials for replacement of missing or diseased bone. Problems caused by mismatch of mechanical properties between high-stiffness metallic implant and low-stiffness bone have lead to development process of fibre-reinforced composite implants, the mechanical properties of which can be tailored.

The achieving of proper and permanent fixation between bone and the implant is a crucial and challenging task in order to transfer the load within physiological range. Possible fixation methods include: 1) mechanical interlocking, which is achieved by press-fitting the implant by using bone cement as a grouting agent, 2) biological fixation, which is achieved by making the surface of the implant rough or porous and allowing bone to grow into the structure and 3) direct chemical bonding between implant and bone by coating the implant e.g. with hydroxyapatite or bioactive glass (Park *et al.*, 2007).

2. REVIEW OF THE LITERATURE

2.1. Bone remodelling and adaptation

Living bone is in a continuous remodelling process in order to adapt to the surrounding mechanical environment. According to Wolff's law of functional adaptation and to the theory of Adaptive Elasticity by Cowin *et al*., bone cells sense chances in the state of strain around them and either increase bone formation or resorption in order to maintain the strain within a limited strain range (Wolf, 1986; Hart 2001, Guo 2001). It has been hypothesised that remodelling signals are related to the piezoelectric properties of bone, which cause bone to generate small electrical potentials under stress (*Becker RO and Marino AA, 1982)*. It has been suggested that two different mechanisms may cause this effect: molecular asymmetry of collagen in dry bone and electrical signals caused by flow of ionic electrolytes through the channels in wet bone (Park and Lakes, 2007). The implantation of prosthetic devices changes the mechanical environment of the host bone and bone remodelling process adapts the structure of bone to this changed situation (Katoozian and Davy, 2000).

The stiffness of conventional metallic implants can be five to twenty times that of bone (Chang *et al.*, 1990; Williams and McNamara, 1987). After the operation, most of the load is carried by the metallic implant, due to its higher stiffness, leaving the bone virtually unstressed. This phenomenon is known as stress-shielding effect. Lack of the mechanical stimuli, which are needed to maintain the structural integrity and morphology of bone, causes bone resorption and loosening of the implant. On the other hand, overloading of bone is also harmful and can lead to creep or fatigue of bone tissue. (Huiskes and Nunamaker 1984; Huiskes *et al.*, 2000; Rubin and Lanyon, 1985).

2.2. Fibre-reinforced composites as potential implant materials

Polymer-matrix fibre-reinforced composites (FRC) have been widely studied in the development of ideal materials for load-bearing endosseus applications (e.g. hip prosthesis). The combination of a convenient selection of material characteristics, such as matrix polymer, type of fibres, fibre orientation, length and volume fraction, allows designing and optimisation of desired mechanical properties of FRC to meet the mechanical behaviour of bone. Proper adhesion of fibres to the polymer matrix is needed to transfer the stresses from the matrix to the fibres. The interface between fibre and polymer matrix is crucial to the fracture toughness and moisture resistance performance of the composite (Vallittu, 1996).

Voigt's equation (the basic rule of mixtures) predicts the modulus of elasticity of the continuous and aligned FRC (E_{cl}) in the direction of alignment as follows (fibre-matrix interfacial bond is assumed to be very good):

$$E_{cl} = E_m(1-V_f) + E_fV_f$$

where E_m and E_f refer to the modulus of elasticity of matrix polymer and fibres, respectively. V_f refers to the volume fraction of fibres. Similarly, the modulus of elasticity for discontinuous and randomly orientated FRC (E_{cd}) is given by the relationship:

$$E_{cd} = E_m(1-V_f) + KE_fV_f$$

where K is the fibre efficiency parameter that depends on V_f and the E_f / E_m ratio. The magnitude of K is usually in the range 0.1 to 0.6. The strength of the continuous and aligned FRC (σ_{cl}^*) in the direction of alignment is described by the following equation:

$$\sigma_{cl}^* = \sigma_f^* V_f + \sigma_m' (1 - V_f)$$

where σ_f^* is the tensile strength of the fibre and σ_m' is the stress in the polymer matrix at fibre failure (Callister, 2007). The critical fibre volume fraction (V_{crit}), i.e. the amount of fibres needed to ensure the strength of the FRC is greater than that of the polymer matrix, can be solved as follows ($V_f = V_{crit}$ and $\sigma_{cl}^* = \sigma_m^*$):

$$V_{crit} = \frac{\sigma_m^* - \sigma_m'}{\sigma_f^* - \sigma_m'}$$

where σ_m^* is the stress at the polymer matrix failure (Bowen et al., 2005). Failure of fibre-reinforced composites is a relatively complex process, and several failure types are possible. The large differences between measured (lower) and estimated (higher) stress values based on the basic rule of mixtures have been observed (Padmanabhan and Kishore, 1995). The disparity between these results is attributed to the large volume of defects (e.g. pores, debonding, cracks) introduced during processing of either fibre or composite. In general, the defect levels up to 30 v% in the polymer matrix have virtually no effect on the strength of the composite whereas a small v% of defects in the fibre profoundly affects the strength (Sarkar, 1998).

Short fibres do not reinforce as effectively as continuous fibres due to fibre end effects in load transfer process, which may reduce the fibre stress. In addition to this, randomly orientated short fibres can not be packed at such high volume fractions as continuous fibres. Under applied tension, the load is transferred by shear at the polymer matrix / fibre interface. At the fibre ends, the strain in the matrix is higher than in the fibre. On the other hand, the tensile stress in the fibre is zero at the fibre ends and increases towards the centre (Callister, 2007).

Some critical fibre length is needed for effective strengthening and stiffening of the FRC. The critical fibre length (L_c) is dependent on the fibre diameter (d), the ultimate strength

of the fibre (σ_f^{max}), and on the fibre-matrix bond strength / the shear yield strength of the matrix polymer (depending whichever is smaller) τ_c according to

$$L_c = \frac{\sigma_f^{max} d}{2\tau_c}$$

When a tensile stress equal to σ_f^{max} is applied to a fibre having a critical length, the maximum fibre load is achieved only at the axial centre of the fibre (Fig.2). The fibre reinforcement becomes more effective when the fibre length is increased. If the fibre length is significantly less than L_c, the polymer matrix deforms around the fibre and there is virtually no stress transfer from matrix to fibres. For many of glass and carbon fibre-polymer matrix combinations, the critical fibre length is on the order of 1 mm. The diameter of the fibre plays an important role in maximising stress transfer. Smaller diameter leads to a greater surface area of the fibre per unit weight and allows enhanced stress transfer (Murphy, 1998a).

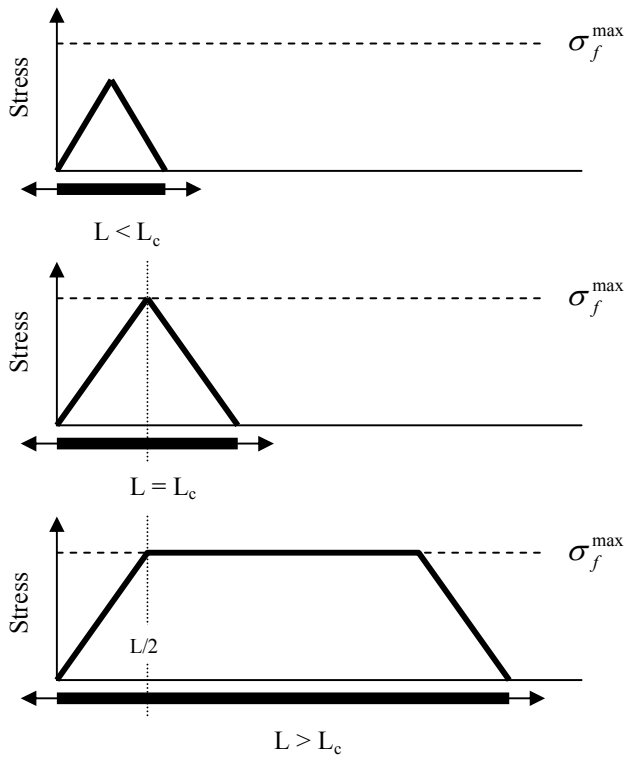

Figure 2. Stress-position profiles depending on fibre length. The figure has been modified from Callister (Callister, 2007).

The average stress in the short fibre is lower than in a continuous fibre due to the low stress at fibre ends. For short fibres (L > L_c) the average stress ($\sigma_f^{\bar{}}$) can be estimated using the following formula (Callister, 2007):

$$\sigma_f^{av} = \sigma_f^{\max}\left[1-\left(\frac{L_c}{2L}\right)\right]$$

The reinforcing efficiency of fibres with different orientations, Krenchel's factor, is presented in Figure 3. Highest mechanical properties will be achieved by using continuous unidirectional fibres ($L > 15L_c$), but only anisotropically (i.e. the direction of applied force and orientation of the fibres should match) (Murphy, 1998a). The mechanical properties perpendicular to the fibre direction may be lower than those values of the matrix alone, because the interface between the fibre and the matrix becomes a critical aspect. The reinforcing efficiency of randomly orientated short fibres is much lower compared to unidirectional fibres, but the short fibres are able to provide a three-dimensional reinforcing effect (Hull and Clyne, 2002).

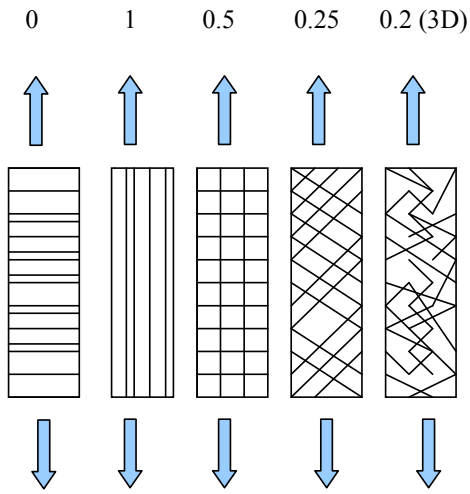

Figure 3. The reinforcing efficiency (Krenchel's factor) of fibres with different orientation. Arrows show the direction of the load. The figure has been modified from Vallittu (Vallittu, 2001).

Possibility to combine e.g. unidirectional fibres and braided-fabric in order to increase shear strength in torsion makes FRCs an attractive alternative for orthopaedic applications as shown in Table 1.

Table 1. Mechanical properties in torsion of FRC implants, conventional Ti6Al4V implants and bone (*Hiermer *et al.*, 1998; ¤Schmitt-Thomas et al., 1998; #Cowin, 2001).

Parameter	***Unidirectional carbon fibre (60 vol%) -epoxy composite****	***Unidirectional +45° braided carbon fibre - epoxy composite****	***Ti-6Al-4V***¤	***Human femur***
Shear strength (MPa)	72.0	198	494	53.1 – 68 #
Shear modulus (GPa)	5.8	4.8	66.3	3.4 - 4.2 ¤

The design of homogenous isotropic metallic implants is focused on geometry, while FRC implants offer a new approach for material-structure based designs. It is even possible to tailor a load transfer pattern between implant and bone by varying the stiffness of the implant not only along its length but also through its thickness by selecting the right reinforcing parameters (De Santis *et al.*, 2004). Metal-free FRCs do not cause artefacts on computed tomography and magnetic imaging. FRCs are nearly radiolucent in radiographs and allow for observation of the bone – implant interface (Kruger et al., 1998).

2.2.1. Non-resorbable resin matrices

Non-resorbable FRCs have been widely studied and developed for various orthopaedic applications such as spine rods, spine disks, intramedullar nails, bone plates and screws, total knee replacements and hip replacements (Fujihara *et al.*, 2004). The requirements for polymer matrices to be used in hard tissue substitution include fatigue resistance, low water absorption, resistance to aging in body fluids, biocompatibility, dimensional stability, absence of harmful leachable products (e.g. residual monomers, activators) and being sterilisable by standard methods (e.g. autoclave, dry heat, ethylene oxide, gamma irradiation) (Eschbach, 2000).

Potential non-resorbable polymer candidates for hard tissue replacement include polyether-etherketone (PEEK), polysulfone (PSU), polyetherimide (PEI), epoxy resins, polymethyl methacrylate (PMMA), ultra-high-molecular weight polyethylene (UHMWPE), polyurethane (PU), polypropylene (PP) and liquid crystalline polymer (LCP). (Ramakrishna *et al.*, 2001; Mano *et al.*, 2004). The most promising and recently widely studied polymer matrix candidates for orthopaedic applications are PEEK, PSU, PEI, epoxy resin, PMMA and bisphenol A glycidyl methacrylate (Bis-GMA)-based resin systems.

PEEK has excellent mechanical stability in physiologic saline (Zhang *et al.*, 1996). In addition to this, PEEK is highly stable against ionizing irradiation and even long time dry heat or steam sterilisation has no adverse effects on the mechanical properties. PEEK is insoluble in common solvents and has high resistance to wear and dynamic fatigue (Eschbach 2000). PEEK compounds have good biocompatibility (Wenz *et al.*, 1990; Morrison *et al.*, 1995). Processing conditions of PEEK are critical due to its semi-crystalline structure (Eschbach 2000). Due to high viscosity of PEEK and limitations in material selection, textile composites using PEEK as matrix polymer have not has their large scale breakthrough (Fujihara *et al.*, 2004a). Micro-braiding fabrication technique, which may be applied to several orthopaedic applications, has been developed to overcome difficulties in fabrication process (Sakaguchi *et al*., 2000). A lot of effort has also been put in developing macro-braided and knitted carbon fibre / PEEK composites (Fujihara *et al*., 2004b).

PSU is a biologically inert polymer and has a good resistance to sterilization procedures (*Dickinson, 1989)* Cell culture studies have shown that PSU does not interfere with

proliferation in the early stages of bone-forming cells, but prevents the final steps of matrix formation (van Loon *et al.*, 1995). Carbon and Kevlar® fibre reinforced PS composites have shown a dramatic reduction of mechanical properties following saturation in saline. Significant degradation at the interface fibre-matrix interface occurred and the composite experienced a fatigue failure at 10^5 load cycles at applied load level of only 15% of its dry strength (Latour and Black, 1993).

Easily processable PEI has a high resistance to organic solvents, gamma irradiation and autoclave sterilisation. It is non-cytotoxic polymer and an excellent substrate for cell growth (Peluso *et al.*, 1994). It has been shown that carbon/glass fibre reinforced PEI did not induce adverse or inflammatory reaction *in vivo* (Merolli *et al.*, 1999).

Heat-resistant epoxy resins with variable biocompatibility and durability characteristics have found only limited interest in orthopaedic applications, although successful commercial applications in fracture fixation exist. Carefully selected and properly processed epoxy resins can have excellent biocompatibility characteristics (Howard *et al.*, 1985). The prosessability of epoxy resins can also be much better when compared to thermoplastics allowing fabrication of more sophisticated composite structures.

PMMA has been extensively used as bone cement since the late 1950s (Charnley, 1960) but there are some controversies about the bone tissue effects of PMMA. In several studies, fibrous layer formation around PMMA has been observed due to exothermal polymerisation reaction or toxic effect of leachable residual monomers. On the other hand, some authors have observed direct bone contacts with PMMA after 15 days to more than 17 years after implantation of cemented hip prosthesis (Linder and Hansson, 1983; Jasty *et al.*, 1991). Vallittu *et al.* have shown in *in vitro* studies that glass or carbon fibre reinforced PMMA composite have relatively good biocompatibility after being polymerise *ex vivo* (Vallittu and Ekstrand, 1999). However, animal experiment results by Heikkilä *et al*. revealed disturbed bone formation at the surface of PMMA implants consisting of bioactive glass or hydroxyapatite particles (Heikkilä *et al.*, 1995).

Thermoset resin systems based on Bis-GMA have been widely used in restorative dentistry and recently introduced as a potential matrix candidate for craniofacial and orthopaedic applications (Tuusa, 2007; Zhao et al., 2008). Polymerised Bis-GMA-based resin systems are highly cross-linked, have low polymerisation shrinkage and stiff structure (Peutzfeldt, 1997). In some conditions Bis-GMA-based resins can release bisphenol-A which has been found to be estrogenic in breast tumour cell culture studies (Olea *et al.,* 1996).

2.2.2. Fibre reinforcements

The mechanical properties of the most common fibre reinforcements used in polymeric biomaterials composites are listed in Table 2.

Table 2. Tensile properties of selected fibres (*Lynch, 1989; #Pirhonen, 2006).

Fibre	*Tensile strength (MPa)*	*Tensile modulus (GPa)*
Carbon AS-4*	4000	231
E-Glass*	3450	72.5
Bioactive glass 13-93 (dry)#	862	
Aramid (Kevlar™ 49)*	2800	138

Carbon fibres are rigid, inert and biocompatible reinforcements that are resistant to stretching, but tend to fail by buckling in compression. Carbon fibres have high resistance to fatigue, creep and wear. The impact strength of carbon fibre composites is lower than that of glass or aramid fibre composites (Murphy, 1998b; Lewandowska-Szumie *et al.*, 1997). The biocompatibility of carbon fibres has been a subject of interest for long time. Early animal experiments with carbon fibres as anterior cruciate construction material at the late 1970s suggested a surprising induction of tissue to produce a neo-tendon or neo-ligament (Jenkins, 1987; Jenkins and McKibbin, 1980). However, later clinical studies revealed widespread fragmentation of the carbon fibres leading to symptoms of synovitis and no evidence of structure resembling neo-ligament was found (Amis *et al.*, 1988; Rushton et al., 1983; Mäkisalo et al., 1989). However, carbon fibres partly embedded in epoxy do not cause adverse effects (Ali *et al.*, 1990a). Recently, much effort has put into developing PEEK-based composites reinforced with fibres for orthopaedic applications, such as bone fixation plates (Veerabagu *et al.*, 2003; Rohner *et al*. 2005).

Glass fibre reinforcements with high tensile and compression strength, low extensibility (3.5%), a relatively high modulus of elasticity and bending strength, have been successfully used in restorative and prosthetic dentistry since the late 1990s. PMMA or epoxy resin -based glass fibre-reinforced composites have also been developed for orthopaedic devises, such as bone plates (Akeson *et al*., 1980; McKenna BB et al., 1980). Glass fibres stretch uniformly under stress to the breaking point without yielding and the removal of the load let the fibre return to its original length. This property enables glass fibres to store and release large amounts of energy (Murphy, 1998b). De Santis *et al.* have developed PEI-based carbon and glass reinforced hybrid composite hip joint prosthesis, whose mechanical properties can be tailored. The glass-carbon hybrid is stronger, tougher and it has a higher impact resistance than either all-carbon or all-glass FRCs. In order to prevent stress concentration at the tip, the region was mainly reinforced with glass fibres and characterised by a relative low elastic modulus (14.3 GPa) (De Santis *et al.*, 2000). Biocompatibility of glass fibres has been studied by Väkiparta *et al*. and no signs of cytotoxicity were found (Väkiparta *et al.*, 2004). Glass fibres have adequate mechanical properties and excellent silane coupling agent promoted bonding properties with resin matrix. The coupling agents are prone to hydrolysis via ester linkages within the molecules or siloxane links that are formed with fibres (Santerre *et al.*, 2001). Reversible process of hydrolysis and reformation of covalent chemical bonds may reduce internal stress in the material when these internal stresses are a result of, for instance, polymerisation contraction (Venhoven *et al.*, 1994). On the other hand,

hydrolysis of silane sizing under extreme conditions of stress and moisture can lead to debonding of fibres from the matrix (Jancar *et al.*, 1993a,b).

Resorbable silica-based bioactive glass fibres have recently been promoted as possible reinforcing materials. Bioactive glasses, exposed to tissue fluids, can form a bonding layer of hydroxyl-carbonate-apatite with an underlying layer of silica gel (Hench and Paschall, 1973). The addition of bioactive glass fibres provide an osteopromotive effect, if the fibres are partly exposed, resulting in higher interfacial bond strength between implant and bone (Marcolongo *et al.*, 1998). However, degradation of bioactive fibres decreases the mechanical properties of the composite. 3-point bending test performed for bioactive glass (13-93) fibres showed a dramatic loss in mechanical properties after being immersed in simulated body fluid for five weeks. Flexural strength dropped from 1443 ± 697 MPa to 285 ± 162 MPa and flexural modulus from 68.1 ± 6.8 GPa to 47.7 ± 10.4 GPa (Pirhonen, 2006). One has to also keep in mind that bioactive glasses in fibre form with increased surface area may behave quite differently compared to bulk bioactive glasses. It has been noticed that the increased surface area for reaction with surrounding tissue and fluids, of sintered bioactive glasses due to microporosity, causes necrosis and mineralisation of tissues (Hench, 1990).

Aramid fibres, such as Kevlar™ (*p*-phenylene terephtalate), have excellent tensile properties but perform poorly in compression. Thus, no suitable applications for aramid fibres have been found in hard tissue replacement, because orthopeadical implants are predominantly loaded in bending (Evans *al.*, 1998). However, recent studies of three-dimensional braided carbon/Kevlar™ fibre hybrid composites have revealed positive deviation from the rule of mixture (i.e. Voigt's equation). It was assumed that stiff carbon fibres could prevent Kevlar™ fibres from buckling and presence of Kevlar® fibres could increase damage tolerance of carbon fibres leading to a higher bending strength of the composite (Wan *et al.*, 2005).

2.3. Bone-implant interface

The successful osseointegration (Brånemark 1952) depends on implant material selection, surface properties (i.e. surface chemistry and microgeometry) of the implant and mechanical conditions at the implant-bone interface. Micromotions (Søballe *et al.*, 1992), abrasion of wear particles (Huiskes and Nunamaker, 1984) and stress shielding at the interface can inhibit bone incorporation with the implant. Wear debris activate macrophages which activate osteoclasts and initiate bone resoption (Sundfeldt *et al.*, 2006) Micromotion (i.e. small movements between implant and the surrounding bone) due to joint loading is an important factor in progressive interface debonding of cemented and cementless hip prosthesis (Huiskes and Nunamaker, 1984). All of these failure scenarios are interlinked and should be taken seriously when a new prosthetic device is designed (Huiskes *et al.*, 1993).

In order to minimise micromotions and to achieve increasing stress shearing with the surrounding bone, fixation between implant and bone must be achieved. One method to promote attachment between implant and host bone is to use implants with interconnecting porous surface structure. Hulbert *et al.* showed that a pore size of 100 μm allows bone ingrowht into porous structure, while pore size greater than 150 μm is needed for osteon formation (Hulbert, 1969). *In vivo* experiment by Bobyn *et al.* revealed that a pore size range of 50-400 μm provided the maximum fixation strength (Bobyn *et al.*, 1980).

The physiological response to implant with interconnective porous surface structure was similar to the healing cascade of cancellous bone defects with new bone formation filling in the voids of the porous layer (Bobyn *et al.*, 1980). Injury during implantation develops a haematoma which is replaced by primitive mesenchymal tissue. The mesenchymal tissue may differentiate into woven bone (after about four weeks) or fibrous tissue. Woven bone is then remodelled to produce secondary lamellar bone or resorbed to form fibrous tissue. The remodelling of woven bone is believed to be influenced greatly by the mechanical environment at bone-implant interface. If too much motion occurs, the ingrown tissue will be collagenous tissue (Galante *et al.*, 1986).

Bone ingrowth into porous surface of the implant stabilises and gives significant strength to the bone-implant interface improving the clinical success (Søballe *et al.*, 1990; Galante, 1988). However, many studies have shown that bone volume fraction within the porous surface layer of the implant is in general less than 35% (Galante and Jacobs, 1992; Cook *et al.*, 1988 and1989).

2.4. Finite element analysis

Finite element analysis (FEA) is a mathematical modelling technique which was first introduced in the orthopaedic literature in the early 1970s (Brekelmans *et al.*, 1972). The FEA has been developed as a powerful tool to determine the failure probabilities of implants (Tanimoto *et al.*, 2004), to predict late aseptic loosening of implant (Taylor *et al.*, 1995), to simulate bone remodelling and ingrowth (Huiskes *et al.*, 1987), and to create new, better functioning implant designs (Yildiz *et al.*, 1998).

The FE models are based on several assumptions, such as acting loads, material properties and the behaviour of the bone-implant interface. Simplifications are also needed, since real phenomena are too complex to be described mathematically. However, the FEA is still a useful tool in the search for possible failure mechanisms or design criteria of composite prosthesis, since it is very cheap compared to laboratory testing methods and animal experiments.

FEA results predicting initial contact conditions revealed that low-stiffness implants had similar deformations to that of the surrounding bone. Therefore, peak stresses were reduced, leading to more homogenous shear stress distribution with stress values closer to physiological range at the interface of composites compared to titanium implants

(Simon *et al.*, 2003). However, micromotions were larger in magnitude and covered larger areas with the composite implant than with the titanium implant, but were within a range of acceptable values (less than 50-100 μm) for osseointegration as verified with histological findings. (Simon *et al.*, 2003; Szmuckler-Moncler *et al.*, 1998).

Implants with low stiffness have a smaller load-bearing capacity and therefore may cause excessive stresses at the bone-implant interface, which leads to debonding of the implant. (Huiskes and Nunamaker, 1984). Katoozian *et al.* have used the FE method to minimise stress/strain concentrations at the bone-implant interface by optimising orientation and volume fraction of carbon fibres in PEEK composite (Katoozian *et al.*, 2001).

2.5. FRCs in clinical studies

Although carbon fibres are no longer used for ligament reconstruction it is still widely studied as reinforcements of FRCs intended to use as orthopaedic and spinal devices, such as compression plates, stems of the hip prosthesis and spinal fusion cages. Carbon fibre reinforced PEEK-composites have recently found their commercial applications as osteosynthesis plates, cervical plates, screws (Icotech AG, Switzerland), intervertebral spacers (Icotech AG, Switzerland and Signus Medizintechnic GmbH, Germany), translaminar pins (Icotech AG, Switzerland and Signus Medizintechnic GmbH, Germany) and interbody fusion cages (Zimmer Spine Inc. USA and DePuy Spine Inc., USA).

Carbon fibre-reinforced epoxy resin impregnated laminates were used to fabricate composite bone plates. Forty forearm bone fractures in 29 patients, mean age of 26 years, were fixed with these FRC plates and stainless steel screws. No mechanical failures of FRC plates or non-unions of the bone fracture lines were observed. At removal of FRC plates, in five of the 40 fracture sites, there was some reaction with opalescent free fluid and gelatinous granulation tissue. Soft tissue specimens revealed carbon fibre fragments lying in the fibrous tissue together with a few giant cells. In comparison with retrospective clinical trials by same authors, no statistically significant increase in the rate of union was observed in the case of FRC plates compared to metallic plates. On the other hand, the use of less stiff FRC plates speeded up the formation of abundant external callus providing additional stabilisation of the fracture and also allowing normal activity of the patient much earlier (Ali *et al*., 1990b). Pemberton *et al*. did not observe any granulation tissue formation or evidence of acute inflammatory reaction caused by carbon fibre-reinforced epoxy bone plates in the clinical study that included nineteen 16–80-year-old patients (mean age of 44 years) with fractures complicated either by poor bone quality, non-union, comminution or infection. Increased callus formation due to the stress-shearing between plate and the bone made it possible to accept gaps and to avoid the use of supplementary bone grafts in the comminuted fractures. Poor bone quality may be also one reason to use FRC plates and screws instead of conventional metallic ones, because screws have the tendency to loosen. Despite many advantages of FRC bone plates compared to metallic plates, the impossibility to reshape the FRC

plate at the time of surgery in order to adapt it to the anatomy of the patient might be considered as a disadvantage (Pemberton *et al*., 1992).

Cementless total hip arthoplasties using anatomically shaped press-fit fibre-reinforced epoxy stem of the hip prosthesis were performed by Adam *et al*. in 48 patients aged 30–70 years (mean age of 59 years). The roughness of proximal part of the FRC stem was obtained by interlaced carbon fibres. At 12 months post-operatively, 27% of patients reported thigh pain and poor function of the hip. Early aseptic loosening was detected in 4% of the cases. At six years, macroscopic loosening of the FRC stem was observed in 92% of hips. The stems were completely covered with fibrous tissue without any bone ongrowth. No stem breakage, carbon fibre wear, inflammatory reactions or osteolysis around the FRC stem were observed. Bad stem design was found to be responsible for prosthesis failure. Sufficient primary rotation stability of the stem was hard to achieve due to non-optimal stem size and shape. The proximal part of the stem was too smooth for bony fixation. Unphysiological diaphyseal load also caused a massive cortical thickening (Adam *et al*., 2002). Another attempt to perform a total hip arthoplasty using continuous carbon fibre -reinforced PSU composite stem was reported in a case study by Allcock *et al*. At 30 months after surgery, the neck-body junction of the FRC stem was cracked and carbon fibres were torn apart. Tendency to fail by buckling in compression and greater proximal micro motions due to reduced stiffness might have caused the fatigue failure of the carbon fibre -reinforced composite stem (Allcock *et al*., 1997). Fully porous coated composite hip replacement stem including the core created from a cobalt-chromium-molybdenum alloy, the middle segment made from polyaryletherketone (PAEK) and the outer layer composed of a mesh of commercially pure titanium fibres (Epoch®, Zimmer Inc., USA) indicated excellent clinical success with the evidence of osseus ingrowth, ongrowth and integration in the intermediate-term follow-up study (6.2 years) (Akhavan *et al*., 2006).

To overcome the shortcomings of the autograft and allograft -related risk of transmissions of infectious diseases, an effort has been made in the development of FRC materials for interbody fusion cages. A hundred patients, men and women, who ranged in age from 19 to 82 years (mean age of 49 years) suffering from cervical spondylosis or soft-disc herniation, were included in the retrospective clinical study by Salame *et al*. Composite fusion cages made of continuous carbon fibre -reinforced PEEK with a shape of trapezoidal hollow box were packed with the bone graft and implanted into the disc space. The follow-up time varied from 12 to 40 months. No cases of displacement, breakage or other-FRC fusion cage -related complication were observed and immediate and adequate vertebral stability was maintained until solid fusion developed. The possibility that bone graft might be unnecessary was raised due to observations concerning the new bone growth from the adjacent endplates rather than form the bone graft (Salame et al., 2001). However, clinical study with 36 patients (mean age of 47 years) performed by Schils *et al*. showed no superior results in the empty carbon fibre -reinforced composite cage group, the absence of donor site morbidity and significantly shorter operative times were definitive advantages compared to outcomes in the autograft filled fibre-reinforced composite cage group (Schils et al., 2006).

3. AIMS OF THE PRESENT STUDY

This study was an attempt to develop a method to fabricate fibre-reinforced composite (FRC) with a dense load-bearing core and porous surface in order to eliminate or decrease stress-shielding effect and promote fixation between bone and the implant. Based on preliminary investigations the hypothesis was that solvent treatment of the FRC would create a porous surface layer. Another objective was to characterise the porous surface in order to find out, if the material would be suitable to be used as a load-bearing endosseus implant.

The specific aims of the four studies were:

I To develop the fabrication process for FRC with porous surface and to characterise the pore size and distribution and also the penetration depth of the solvent.

II To evaluate the load-bearding capacity and potentially harmful leachable residual monomer content of FRC with porous surface.

III To evaluate the interfacial strength between bone and FRC implant with porous surface *in vivo* and to analyse stress distribution using finite element method.

IV To examine repair of segmental bone defect *in vivo* using FRC implant with porous surface.

4. MATERIALS AND METHODS

4.1. Materials

The materials used for fabrication of the test specimens and the implants in the studies are listed in Table 3.

Table 3. Materials used in the studies.

Brand	*Manufacturer*	*Type of material*	*Study*
Palapress® powder (clear)	Heraeus Kulzer GmbH & Co KG, Hanau, Germany	PMMA powder[a]	I, II, III, IV
Methyl Methacrylate	Fluka Chemie GmbH, Buchs, Switzerland	Monomer	I, II, III, IV
N,N-Dimethyl-p-toluidine 99%	Sigma-Aldrich Chemie GmbH, Steinheim, Germany	Activator	I, II, III, IV
Stick®	Stick Tech Ltd, Turku, Finland	Preimpregnated E-glass fibres[b]	I, II, III, IV
Tetrahydrofuran	Sigma-Aldrich Laborchemicalien GmbH, Seelze, Germany	Solvent	I, II, III, IV
BAG granules	Vivoxid Ltd, Turku, Finland	Biocative glass (S53P4)[c] granules, size 315-500 µm	IV

[a]Poly(methylmethacrylate-co-methacrylate) copolymer, M_w 220.000. Product contains benzoyl peroxide as a radical initiator.

[b]silanated E-glass fibres with polymethylmethacrylate preimpregnation. The diameter of individual fibre was approximately 16 µm. The main components of E-glass (electrical glass) were SiO_2 54 wt%, CaO 24 wt%, Al_2O_3 14 wt%, B_2O_3 6 wt%. In addition, E-glass contained also small amounts (< 1.0 wt%) MgO, Na_2O and K_2O, as stated by manufacturer.

[c]chemical composition of S53P4 bioactive glass: SiO_2 53 wt%, Na_2O 23 wt%, CaO 20 wt% and P_2O_5 4 wt%.

4.2. Methods

4.2.1. Development of fabrication method for FRCs with porous surface (Studies I-II)

In study I, a method to fabricate polymethylmethacrylate (PMMA) -based composites with randomly orientated short E-glass fibres and porous outermost surface layer was developed. Three groups of composites with various quantities of short E-glass fibres were prepared as follows. Two grams of PMMA powder (Palapress®) containing benzoyl peroxide as a radical initiator and two grams of methylmethacrylate (MMA) monomer containing 2 wt-% N,N-dimethyl-p-toluidine as an activator were mixed together (liquid-to-powder ratio 1:1). Varying quantities, i.e. 0, 5 and 10 wt-% of polymethylmethacrylate preimpregnated E-glass fibres (length: 2-3 mm) were inserted into a syringe (ONCE single use syringe, CODAN Medical ApS, Rødby, Denmark) to fabricate cylindrical specimens (diameter: 12 mm, height: 20 mm). The PMMA-MMA mixture was poured into the syringe and the mixture was polymerised in a pressure-curing device (Ivomat, Typ IP 2, Ivoclar AG., Schaan, Liechtenstein) at a pressure of 400 kPa, at a temperature of 90±3°C, for 20 minutes.

The cylindrical specimen was taken out of the syringe after polymerisation and put into the tetrahydrofuran (THF) solvent for 1, 2, 4 or 6 hours in order to obtain swelling and dissolution of the PMMA on the surface of the specimen at room temperature. A porous surface for the test specimen containing PMMA and glass fibres was obtained by solidification of the swollen and dissolved PMMA layer and evaporation of the solvent THF. The process was considered an interfacial porosity formation process (IPF) because the existence of the glass fibres and their interface with the polymer matrix were found to be crucial for porosity formation in the preliminary investigation. Specimens and implants fabricated for different test purposes are listed in table 4.

Figure 4 represents fibre-reinforced composite (FRC) before and after the solvent treatment. μCT image of fibre orientation and surface porosity of the composite are also shown. Test specimens and implants used in different studies are shown in Figures 5, 6 and 7.

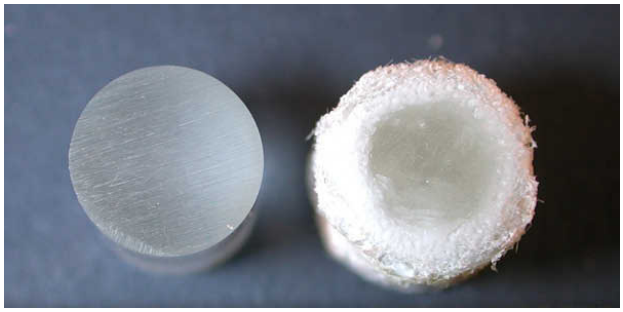

a)

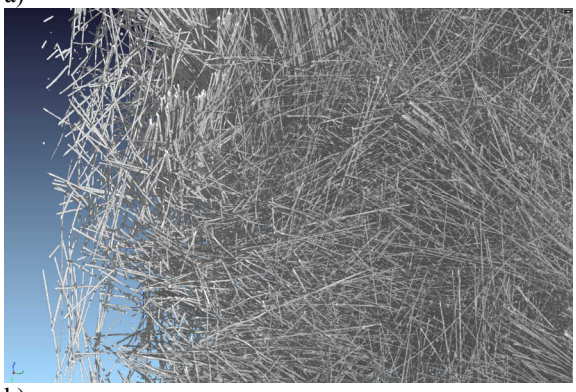

b)

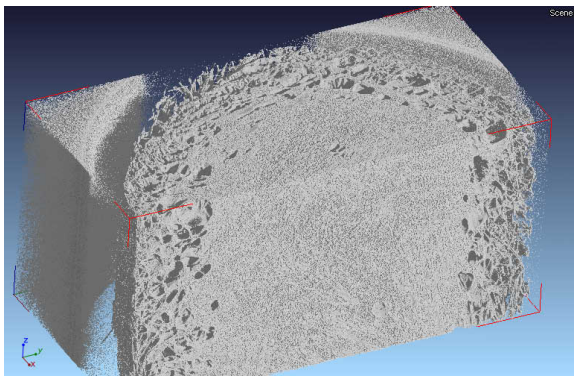

c)

Figure 4. a) FRC before and after solvent treatment, b) µCT image of the FRC with randomly orientated short E-glass fibres (Courtesy of Gissur Örlysson, Innovative Centre Iceland). c) µCT image of a FRC with three-dimensionally continuous porous surface structure (Courtesy of Gissur Örlysson, Innovative Centre Iceland).

Table 4. Specimens and implants fabricated for different test purposes.

Study	*Test method*	*Type of the specimens/implants*	*Dimensions of the specimens/ implants*	*Number or the specimens or implants / test group*
I	Determination of the depth of the porous surface layer by SEM	Twelve groups of specimens: - 0, 5 or 10 wt% of fibres - solvent treatment time 1, 2, 4 or 6 h	Discs[a]: Ø = 12 mm, h = 2 mm	5
I	Vickers micohardness measurements	Eight groups of specimens: - 5 or 10 wt% of fibres - solvent treatment time 1, 2, 4 or 6 h	Discs[a]: Ø = 12 mm, h = 2 mm	5
II	Push-out tests	Three groups of specimens: - PMMA with smooth surface - polymer only, two grooves (groove depth: ~ 0.5 mm) drilled horizontally around the specimens - FRC with porous surface[b]	Cylinders: Ø = 8.6 mm (polymer only specimens) or 8.3 mm (composites), h = 10 mm	12 (+ 3 composite specimens with porous surface for SEM observations)
II	Residual monomer analysis	Four groups of specimens: - 0 or 10 wt% of fibres - solvent treatment time 0 or 1h	Cylinders: Ø = 8.6 mm (polymer only specimens) or 8.3 mm (FRC), h = 5 mm	5
III	Animal experiment, follow-up time: 3, 6 and 12 weeks	Three groups of implants[c]: - PMMA implants with solid surface (Ra = 2.12 ± 0.18 µm) - FRC with porous surface[b] - titanium (Ti)[d] implants with solid surface (Ra = 2.72 ± 0.27 µm)	Rods: Ø = 5.3 mm, h = 10 or 15 mm depending on location of implantation	5-6 implants / group / follow-up time (+ 1 implant/ each group for SEM observations)
III	Finite element analysis	Six groups of implants: - PMMA implants with solid and porous surface - FRC with solid and porous surface - Ti [d] implants with solid and porous surface	Rods: Ø = 5.3 mm, h = 5.2 mm	
IV	Animal experiment, follow-up time: 4, 8 and 20 weeks	Two groups of implants[c]: - PMMA[e] - FRC implants with porous surface and BAG granules[b]	Cylinders (Ø = 8.3 mm, *l* = 10 mm) with intramedullar canal (Ø = 3 mm)	4-6 implants / group / follow-up time

[a]Cylindrical specimens were cut into slices of about 2 mm thickness perpendicular to their long axis, and polished with 1200 grit silicon carbide grinding paper using a grinding machine (LaboPol-21, Struers A/S, Rødovre, Denmark).

[b]Based on results obtained from study I, FRCs with porous surface were fabricated in the same way containing 10 wt% of short E-glass fibres for the studies II, III and IV. THF solvent treatment time was one hour.

[c]All implants were stored for 24 hours at 37°C in distilled water to wash out the residual solvent and MMA monomers. The implants were sterilized in autoclave before surgical operation at temperature of 120°C, pressure of 0.1 MPa for 20 minutes.

[d]Commercially pure titanium, grade 2

[e]Control PMMA implants were fabricated in Laboratory of Polymer Technology, Helsinki University of Technology, Finland. Surface on the implants were roughened with a metallic file.

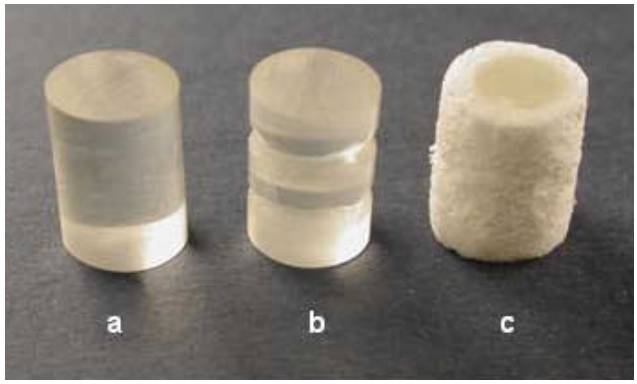

Figure 5. The test implants used in the push-out tests (II): a) smooth surface b) grooved surface and c) porous surface. The implant with porous surface contained 10 wt% of chopped E-glass fibres and the IPF-process.

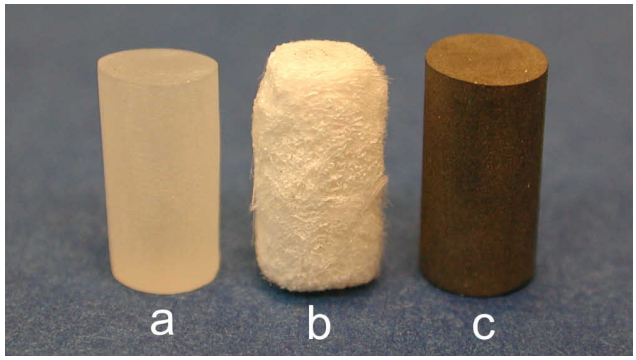

Figure 6. Implants used in study III (Ø = 5.3.mm, l = 10 or 15mm). a) solid PMMA (Ra = 2.12 ± 0.18 µm), b) FRC with porous surface (thickness of the porous surface layer: 300-500 µm, maximum pore size: 500 µm), and c) solid Ti (Ra = 2.72 ± 0.27 µm).

Figure 7. FRC implants with porous surface for segment defect construction in study IV (Ø = 8.3 mm, *l* = 10 mm, intramedullar canal Ø = 3 mm).

4.2.1.1. Scanning electron microscopy, SEM, observations (Studies I-III)

All samples for scanning electron microscope (SEM) observations were coated with a gold layer using a sputter coater (BAL-TEC SCD 050 Sputter Coater, Balzers, Liechtenstein). In study I, the thickness of the porous surface layer of the FRC specimen was measured by a SEM (JSM-5500, JEOL, Tokyo, Japan). SEM micrographs (× 50) of five specimens from each group were taken for visual analysis of the porous structure to determine the average pore size of the surface layer of the specimen.

In study II, visual SEM analysis was performed on three samples in order to illustrate the penetration depth of the dental stone, a material used to simulate bone growth, into the porous surface of FRCs. In study III, the surface textures of all implants were examined by a SEM before animal experiment.

4.2.1.2. Vickers microhardness measurements (Study I)

To evaluate the penetration depth of the THF solvent into the polymer matrix of the core, surface microhardness measurements were made with the slices of the specimen as described above. The microhardness measurements were performed with Duramin-1 Hardness Tester (type 565, Struers A/S, Rødovre, Denmark) at room temperature. The Vickers microhardness test uses a square based pyramidal indenter with an apex of Ø = 136°, producing a diamond shaped indent on the surface. The expression for Vickers hardness number (VHN) is

$$\mathrm{VHN} = 1.854\frac{F}{d^2}$$

Where F is the applied load (N) and d (mm) is the mean diagonal length of the diamond-shaped indent. A press load of 245.3 mN, a press time of 15 s, and a holding time of 5 s after completing the indentation, were used. Individual Vickers microhardness values were calculated as a mean value over five indentations. Special care was taken to measure the surface microhardness of the polymer matrix part only.

4.2.1.3. Residual monomer analysis (Study II)

For the residual monomer analysis, twenty specimens containing 0 and 10 wt% of short glass fibres were prepared as described above. To analyse the release of residual MMA (Fig. 8) from the test specimens (n = 5), the specimens were incubated in 10 ml of deionised Milli-Q water (electrical resistivity 18.2 MΩ cm) at the temperature of 37°C for up to 2 weeks.

After the predetermined storage period of 1, 3, 7 and 14 days, the MMA content of the immersion water was analysed by Shimadzu's (LC-2010) Modular High Performance Liquid Chromatograph (HPLC) system (Shimadzu Corporation, Kyoto, Japan). The incorporated columns used in the system were Phenomex's C18 precolumn (Phenomex, Torrance, CA, USA) and Phenomex's C18 analysis columns (type: RP18, length:

150 mm, internal diameter: 2 mm, particle size: 5 µm). The analysis was carried out as an isocratic run, in which the flow rate was 0.3 ml/min and the mobile phase was methanol:water (70 vol% / 30 vol%) (Methanol HPLC grade, Rathburn Chemicals Ltd, Walkerburn, Scotland). The wavelength of UV light used was 205 nm.

The MMA concentration was measured by HPLC analysis using a standard calibration curve ($R^2 > 0.97$) in which MMA concentrations of 1, 3, 5 and 10 µg/ml served as calibration samples. The concentrations of MMA were calculated from the areas under the curve at the peak produced by the MMA. The amount of released MMA was estimated in ppm per 1.00 g of PMMA per day during the storage period. After the residual monomer analysis, PMMA of the FRCs was combusted at +700°C for one hour and the fibre content (wt%) was calculated from the initial weight of the implant. The weight of the glass fibres was excluded from calculation of the release of residual MMA from the specimens that contained fibres.

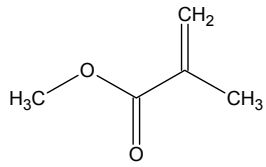

Figure 8. Methyl methacrylate.

4.2.2. Load bearing capacity of FRCs with porous surface (Study II)

Dental stone was used as a simulated bone model in the push-out test. All specimens were first treated with a surface tension decreasing agent and then embedded into the dental stone (GC Fujirock® EP) using the powder-to-liquid ratio of 100 g powder / 20 ml water recommended by the manufacturer. Excess dental stone extending on the top of the specimen was removed using SiC paper and a grinding machine (LaboPol-21, Struers A/S, Rødovre, Denmark). Specimens were left to set for three days at room temperature.

The push-out test for the specimens embedded into dental stone (Fig. 9) was performed on a universal testing machine (Lloyd, model LRX, Lloyd Instruments, Fareham, England) at a loading speed of 1 mm/min, and a force-displacement curve was recorded. Twelve specimens from each group were used for determining the maximum push-out force (N). The clearance of the hole in the support jig was at least 0.8 mm for all specimens.

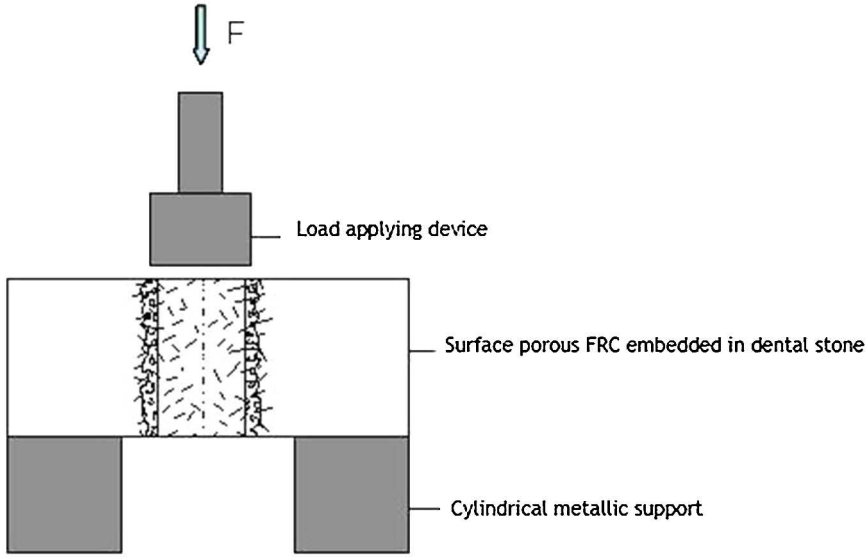

Figure 9. The test sep-up for push-out test.

4.2.3. Animal experiments (Studies III & IV)

The animal experiments were approved by the Lab-Animal Care & Use Committee, the Central Animal Laboratory, the University of Turku and the State Provincial Office of Western Finland (permission no. 51124/7624 and 1345/03).

New Zealand White mature female rabbits weighing 3.0–4.1 kg were used as test animals. General anesthesia by midazolam (Dormicum® Roche Oy, Espoo, Finland) 1.5 mg/kg i.m. and medetomidine (Domitor® Orion-Yhtymä Oyj, Espoo, Finland) 0.25 mg/kg i.m. and ketamine (Ketalar® Pfizer Oy, Espoo, Finland) 15 mg/kg i.m. was used, the operational area was shaved and surgery was performed in sterile operating conditions. Incisions were closed with interrupted absorbable polyglycolic acid sutures (Dexon®, Tyco Healthcare UK Ltd., Gosport, UK) and uninterrupted polyamid sutures (Ethilon®, Johnson & Johnson Intl., Brussels, Belgium).

After operation, the rabbits were placed in cages, given post-operative doses of buprenorphine (Temgesic® Schering-Plough Europe, Brussels, Belgium) 0.015 mg/kg s.c. for three days and allowed unrestricted movement at all times. At pre-selected time-points the rabbits were sacrificed with an overdose of pentobarbital (Nembutal®, Orion Oyj, Espoo, Finland).

4.2.3.1. Surgical procedures

Study III

Eighteen rabbits were used in study III. The follow-up times in the studies were 3 and 6 weeks for FRC and PMMA implants, and 12 weeks for all implant types including the control Ti implant.

The cortical surface of the distal part of the left femur and the proximal part of the left tibia were exposed through the anteromedial approach. Holes (5.3 mm) were drilled using dental burr, with sterile physiological saline irrigation transversally through the intercondylar area of the bone. One randomly selected implant (n = 5-6 implants/type/follow-up time) was inserted into each femur (length of implant: 15 mm) and tibia (length of implant: 10 mm).

Study IV

Twenty-eight rabbits were used in study IV. The follow-up times were 4, 8 and 20 weeks. One rabbit from the FRC group (20 wk) was excluded due to failed alignment of the implant.

The total critical size segment defect, 10 mm in length, was created on the proximal portion of the left tibia with a water-cooled surgical drill. The defect was reconstructed with porous FRC or control PMMA implant and fixed with a titanium plate and screws (Fig. 10).

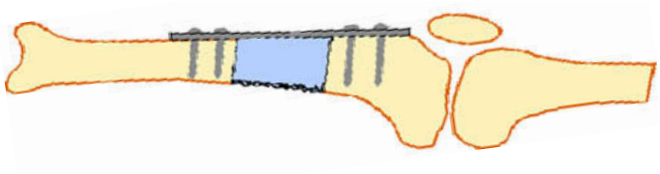

Figure 10. Schematic illustration of positioning and fixation of the implant into the rabbit tibia (Courtesy by Prof. Allan Aho).

4.2.3.2. Determination of fixation between bone and porous FRC (Study III)

Fresh bones were separated from the surrounding tissue and cut into two blocks (Fig 11). One part (l = 5.2 mm) of the block was used in push-out test which was performed on a universal testing machine (Lloyd, model LRX, Lloyd Instruments, Fareham, England). A metal plunger (Ø = 5.0 mm) was used to push-out the implant. The constant loading speed was 1 mm/min and the force-displacement curve was recorded. The clearance of the hole in the support jig was at least 0.8 mm for all implants. Five or six implants from each group were used for determining the maximum shear force (N).

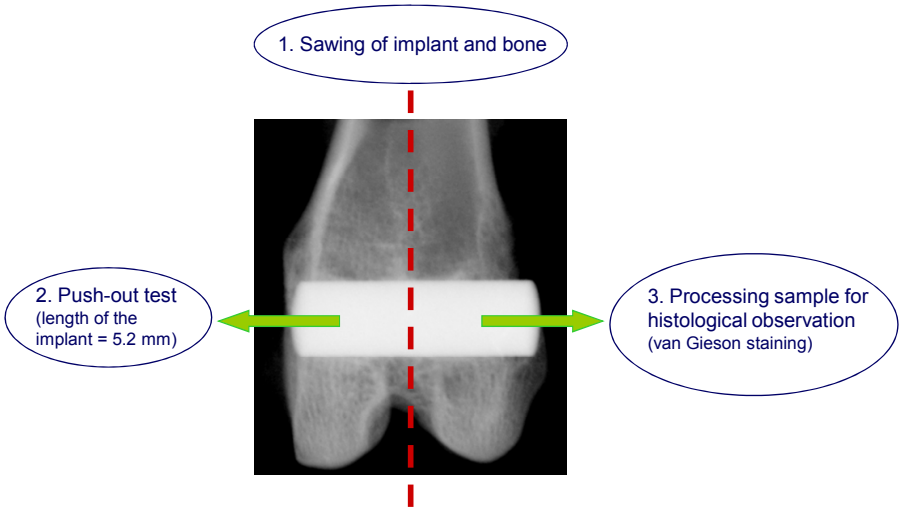

Figure 11. The steps in processing of samples for push-out tests and histological analysis in study III.

4.2.3.3. Histological evaluation (Studies III & IV)

The remaining part of the block from the push-out test in study III and harvested bone blocks in study IV were fixed with 70 % ethanol, dehydrated in increasing ethanol series and embedded in methyl methacrylate resin (Technovit 7200, Exakt Kulzer GmBH, Norderstedt, Germany). Non-decalcified histological sections (20 μm) were prepared through the longitudinal axis of the implants using standard cutting-grinding method (Exakt Apparatebau, Hamburg, Germany).

In study IV, remaining blocks from the preparation of histological slides were stored for microradiographic analysis. Sections (III & IV) were stained with van Gieson method and evaluated by light microscope. Wide-field imaging of histological slides was acquired with Zeiss® Axiovert 200M microscope equipped with an AxioCam MRc5 colour camera. Data was recorded with AxioVision 4.3 software using MosaiX option. Histological evaluations consisted of the examination of tissue on the bone-implant interface and presence of inflammatory reaction.

4.2.3.4. Histomorphometric analysis (Study IV)

In study III, computer assisted histomorphometric analyses were performed with image analysis software (Leica® Qwin v3.00., Leica Microsystems GmbH, Wetzlar, Germany). The thickness of fibrous capsule around the solid PMMA (n = 5) and Ti (n = 5) implants were measured 12 weeks post-operation. In study IV, another imaging analysis software (Microscale TC, Digithurst Ltd, Royston, UK) was used to measure bone growth at different anatomical areas: longitudinal surfaces, junctions (interface) between the implant and cortical host bone, and intramedullar canal. Figure 12 represents the schematic model showing the different areas included in the histomorphometrical measurements.

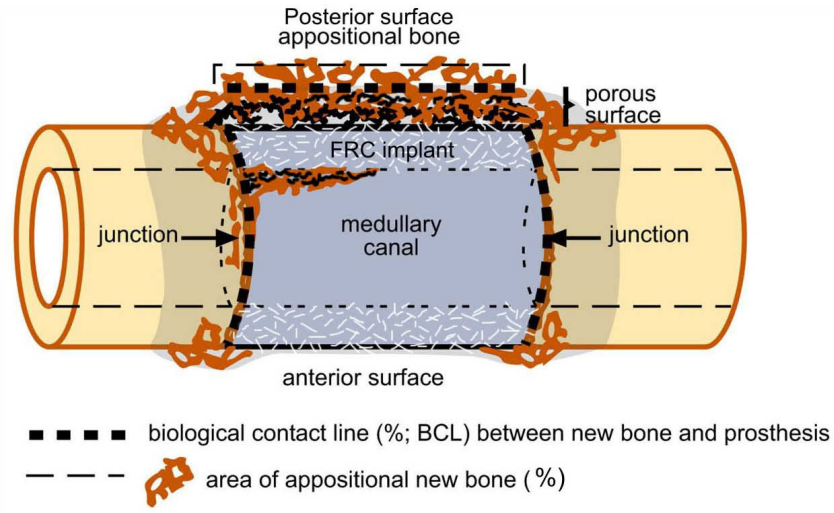

Figure 12. Schematic model showing the different areas included in the histomorphometrical measurements (Courtesy of Prof. Allan Aho).

Total appositional bone growth percentage areas (ABG, area%) over the posterior and anterior surface and also into intramedullar canal (IMG, area%) were measured. The bone contact index (BCI, %) is the percentage from the sum of measured contact lines in millimetres between bone and the implant at cortical junctions, intercortical area, posterior and anterior surface.

4.2.3.5. Microradiographic analysis (Study IV)

Sections (1 mm) for microradiographic analysis were cut through the longitudinal axis of the implants using the remaining blocks from the preparation of histological slides. Faxitron Specimen Radiography System (MX-20, Faxitron X-ray Corporation, Wheeling, USA) was used to expose the specimens for X-rays for 25s with a tube charge of 25 kV and 25 mA. Total appositional bone growth percentage areas (ABG, area%) over the posterior and anterior surface and also into intramedullar canal (IMG, area%) were measured with ImageJ image processing program developed at the National Institutes of Health.

4.2.4. Finite element analysis, FEA (Study III)

The FE models were used to compare the effect of the implant rigidity on shear stress distribution and strain energy density (SED) in order to see what would be the loading scenario of the bone in the pores and in the surrounding of the implant. Three types of materials were used in FEA: PMMA, FRC and Ti, all with both solid and porous surface. Finite element analyses were made with ABAQUS/CAE 6.4-1 using a sub-modeling technique. In this technique, a global model simulating the experimental push-out test was first solved and the result was then used as a loading for the local model representing the true microstructure of the porous surface layer. Both models were axisymmetric.

The geometry of the implants was the same for all three materials both in the global and local models. The diameter of the implant was 5.3 mm following the experimental push-out test set-up. To take into account the porous surface of the implant in the global model, a layer of 872 µm from the outer surface of the implant was assigned different elastic properties from the core. In the cases of solid implants, this area had the same material properties as the core of the implant. In the cases of implant with porous surface layer, the effective properties of the implant-bone layer were used. Effective Young's modulus and Poisson ratio was determined for the porous layer with a model made from cross-sectional SEM image of the actual porous layer of the FRC implant. This model was created with OOF-program (the Object Oriented Finite element method especially developed at National Institute of Standards and Technology, Center for Theoretical and Computational Materials Science, USA) for modeling the microstructures. The program calculates the effective properties by performing a simple tensile test for the model[n+1]. The mesh of this microstructural area contained 19 628 3-noded triangular elements.

To create the local model, the mesh of the porous microstructure was imported into Abaqus CAE (with OOF2ABAQUS program) and transferred into 6-noded quadratic axisymmetric elements. The local model included areas representing the solid implant core and surrounding bone. The meshes had rigid boundary conditions between each other (TIE-command of Abaqus). The local model assumes that the pores were completely filled with the bone, healing was perfect and the interfaces between bone and implant were rigidly bonded. Material properties used in the models are presented in Table 1 in the original publication. Since the global model assumes that bone is completely filling the pores and their interface is fully bonded, whereas the *in vivo* specimens did have some soft tissue and not a complete fill of the pores. The shear stress was determined with equal force of 66N over the whole diameter of the implant for all cases**.** The global model was fully supported in vertical direction from the bottom area mimicking the actual push-out test.

4.2.5. Statistical analysis (Studies I-IV)

Statistical analyses were performed using the SPSS System (Statistical Package for Social Science, SPSS Inc., Chicago, USA) for Windows. Differences were considered significant at a 95% confidence level.

In study I, the correlation coefficient for the solvent treatment time and thickness of the porous layer was calculated and a comparison of the plotted data of specimens containing 5 wt% and 10 wt% glass fibres, with regard to the thickness of the porous layer, was made with one-way ANOVA.

For determining the push-out forces in study II, the Weibull analysis was carried out using Weibull++ 6.0 (Reliasoft Corporation, USA) with median ranks for estimated fracture probability.

$$P_f = 1 - \exp\left[-\left(\frac{x - x_u}{x_o} \right)^m \right]$$

Where m = Weibull modulus (also known as shape factor), a constant that determines the slope of the distribution function and characterizes the spread of the failure data with respect to x axis. x_0 = characteristic push-out force (i.e. the push-out force level at which 63 % of the implants have failed) and x_u = theoretical failure force (= 0).

The statistical analysis of MMA release was performed using univariate ANOVA, followed by Tukey's post hoc analysis in study II.

In study III, the differences in push-out test between solid PMMA, solid Ti and porous FRC implants were studied and a statistical analysis was performed with univariate ANOVA, followed by Tukey's post hoc analysis. The thickness of fibrous capsule around the solid PMMA (n = 5) and Ti (n = 5) implants were measured and statistical analysis was performed using Mann-Whitney U test in study III.

In study IV, the differences between implants were studied with the nonparametric Kruskal-Wallis test, followed by Mann-Whitney U pair-wise comparison.

6. RESULTS AND DISCUSSION

6.1. Development of fabrication method for FRCs with porous surface (Studies I-II)

In study I, a method for producing a porous surface layer in short glass FRC was introduced. During the preliminary tests to produce a porous surface layer for the PMMA-based fibre-reinforced composite, it was noticed that exposure of the reinforcing fibres played a significant role in porosity formation. The results of the present study using the test specimens without glass fibre inclusions confirm this by showing that no porosity was visible on the surface of these test specimens. It is suggested that the diffusion of the solvent into the polymer matrix is easier at the interface of the reinforcing fibre and the polymer matrix. Based on these findings, the process of making a surface layer in the composites was defined an interfacial porosity formation (IPF).

The thickness of the porous surface layer (300-1500 μm) was dependent on the glass fibre quantity and treatment time of the composite specimen by solvent (Fig. 13 and 14). No porosity formation was observed when the specimens did not contain any glass fibres. The pore size was maximally 500 μm, being optimal for bone ingrowth and vascularisation. The continuous structure of the pores, as examined visually comparing

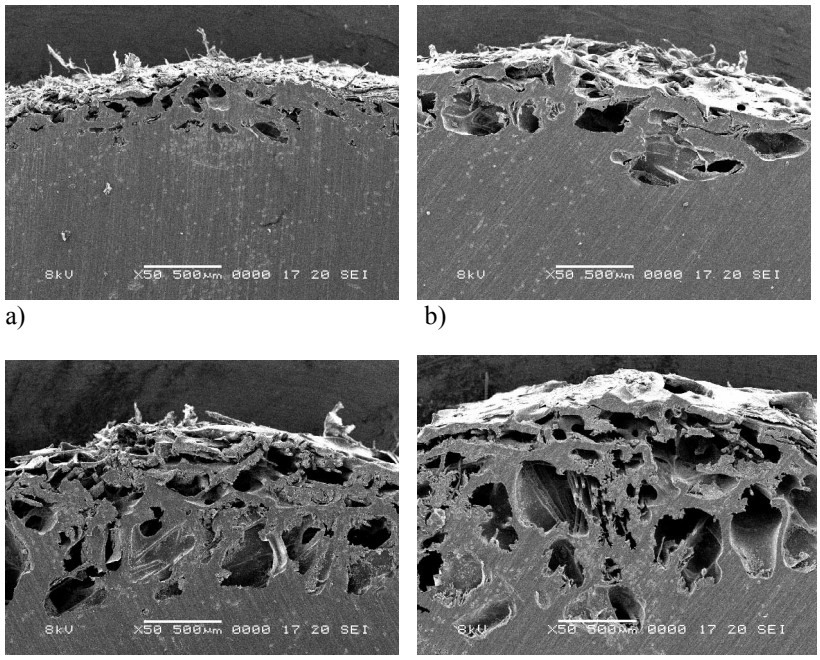

Figure 13. SEM micrographs of the porous surface layer after the specimen containing 10 wt-% of glass fibres had been treated with THF solvent for (a) 1 hour, (b) 2 hours, (c) 4 hours, and (d) 6 hours. Original magnification = × 50. Study I.

the SEM micrographs before and after dental stone impregnation (I and II), is a desired property with regard to bone ingrowth. μCT images also revealed the interconnectivity of the pores (Fig. 4c).

There was a correlation between solvent treatment time and thickness of the porous surface layer (5 wt% of glass fibres: $r = 0.904$, $p < 0.001$; 10 wt% of glass fibres: $r = 0.914$, $p < 0.001$). ANOVA revealed that the thickness of the porous surface layer was higher with 10 wt% of glass fibres than with 5 wt-% of glass fibres ($p = 0.005$).

Possible effects of the THF solvent on the polymer of the core were also examined. It is of great importance to retain the mechanical strength of the glass fibre -reinforced core of the test specimen after the IPF process, because in possible clinical applications, the core behaves as the load-bearing structure of the composite device. The reinforcing effect of the glass fibres is dependent on the adhesion of the fibres to the polymer matrix. The diffusion of the THF solvent seemed to proceed through the interface of the glass fibres and the PMMA. It was hypothesised that the THF solvent could weaken the polymer matrix adhesion to the glass fibres. The result of the surface microhardness measurement showed that the penetration of the THF solvent into the core varies from 0.6 to 1.7 mm, depending on the fibre content and solvent treatment time (Fig 15). Prolongation of the solvent treatment time and an increase in fibre quantity made the interface between the dense core and the porous surface layer clear. Even in the case of the thickest interface layer between the core and the porous surface (obtained with 10 wt% of glass fibres after 1 h of solvent treatment) the length of the glass fibres was enough to provide a mechanical gradient transition from the dense core to the porous surface layer, in which the glass fibres also remained after the IPF process. This could be beneficial from the biomechanical perspective.

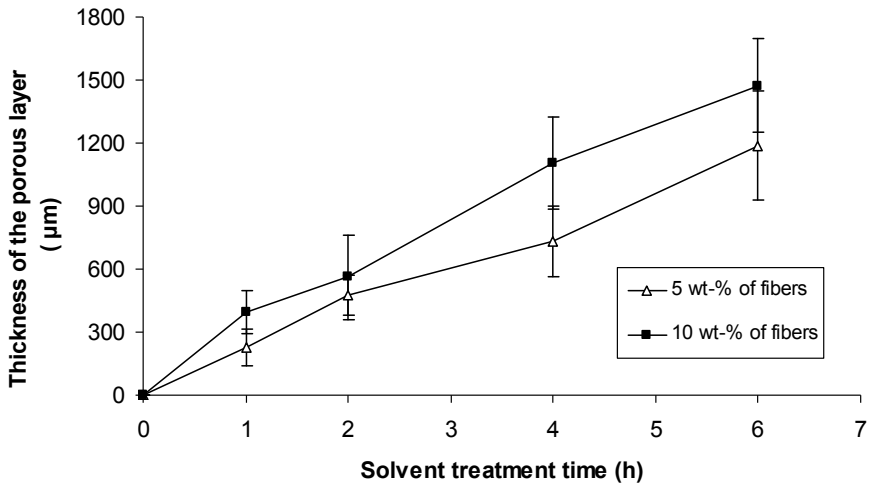

Figure 14. The maximum thickness of the porous surface layer plotted against the THF solvent treatment time with test specimens containing 5 and 10 wt% of glass fibres. Study I.

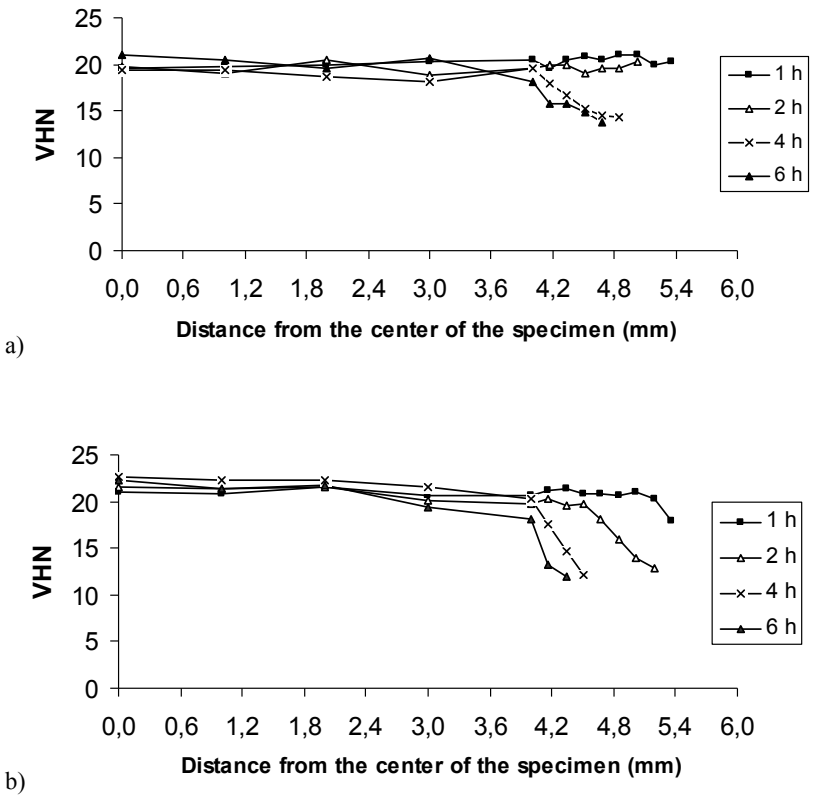

Figure 15. Surface microhardness (VHN) measured from the centre of the cross-section of the test specimen toward the porous surface layer with a) 5 wt-% and b) 10 wt-% glass fibre content, after being treated with THF solvent for various lengths of time. The length of the x-axis (6 mm) represents the radius of the cross-section of the test specimen and the outer boundary of the porous layer. Study I.

Unreacted, leachable monomers can cause chemical necrosis of the tissue (Spealman *et al.,* 1945). Results of residual monomer analysis are presented in Figure 16. The mean residual MMA release per day into water was higher with FRC specimens (with and without the IPF process) than with control implants ($p < 0.001$). The difference diminished with time. Two-way ANOVA revealed that there was some interaction with independent factors of implant type and solvent treatment (IPF process). Results of study II revealed that the majority of residual MMA (125 ppm) leached out from the porous surface FRC implants during the first 24 hours of water storage, while the control implants after solvent treatment without any glass fibre inclusions released only 46 ppm of MMA into storage water. The release of MMA diminished with time. During the 14-day storage period, the total amount of MMA released into water from implants varied between 189 and 379 ppm, depending on the fabrication method of the implants.

The quantity of released MMA was higher in the FRC groups than in control groups. Presence of glass fibres may disturb free radical polymerisation. It was suggested that

void spaces between fibres could serve as oxygen reservoirs and cause internal oxygen inhibition (Vallittu, 1997). Generally, the levels of residual monomers detected were considerably lower than those found in chemically cured fibre-reinforced dentures (Miettinen and Vallittu, 1997). However, total residual monomer content is usually grater than leached monomer content because of the used solvent, i.e. organic solvent vs. water (Inoue and Hayashi, 1982). All implants in studies III and IV were stored for 24 hours at 37°C in distilled water to wash out the residual solvent and MMA monomers.

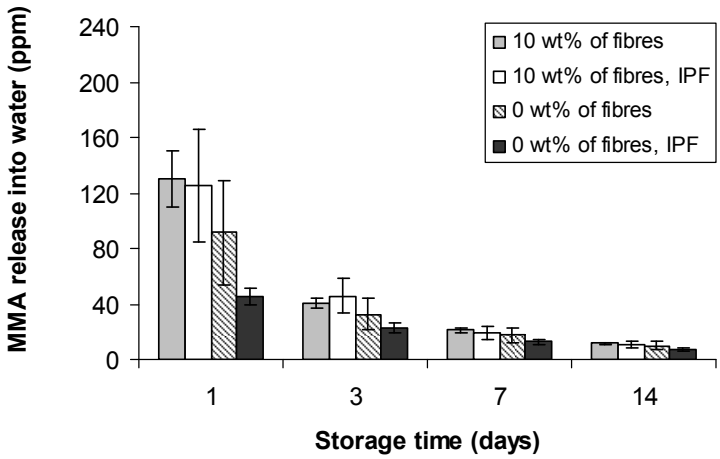

Figure 16. MMA release (ppm) per day. Study II.

In study II the penetration of dental stone, used as a bone model material, into the open pores illustrated that there was an interconnective porous structure in FRC implants which is crucial in terms of bone ingrowth into the material. Some degree of closed porosity was also detected (Fig 17).

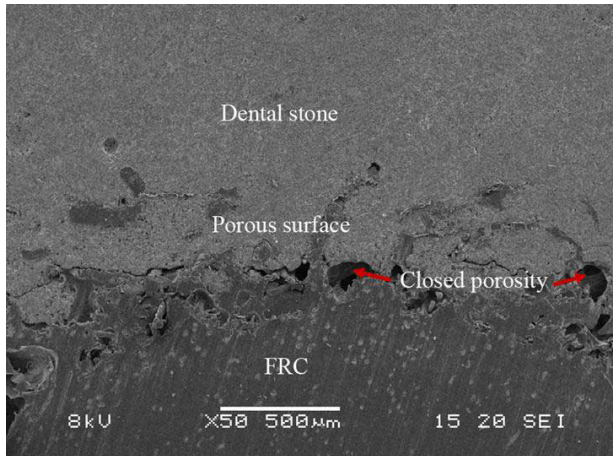

Figure 17. SEM micrographs of surface porous FRC implant after embedding in dental stone and performing push-out test. Study II.

6.2. Load-bearing capacity of porous FRC and bone-implant fixation

It has been shown that the initial fixation of the implant with bone is critical for the use of composite implants, because lower modulus produce higher implant deformations. Histological or radiological methods can not estimate the fixation strength at bone-implant interface. In studies II and III, push-out tests were performed in order to evaluate the load-bearing capacity of fibre-reinforced porous surface layer and to obtain information about fixation between surface porous FRC implant and surrounding tissue.

Before *in vivo* experiments, interlocking between FRC with porous surface and bone simulating material was examined in study II. Penetration of dental stone to surface irregularities was selected to simulate bone ingrowth in the material. The results of the push-out tests are shown in Figure 18. The highest push-out force, 2149 N, was measured for the implants with grooved surface. This value is actually the maximum load value for the gypsum because it cracked up during the test. The push-out force of the surface porous FRC implant was 958 N and the lowest push-out force, 175 N, was measured for the implants with smooth surface.

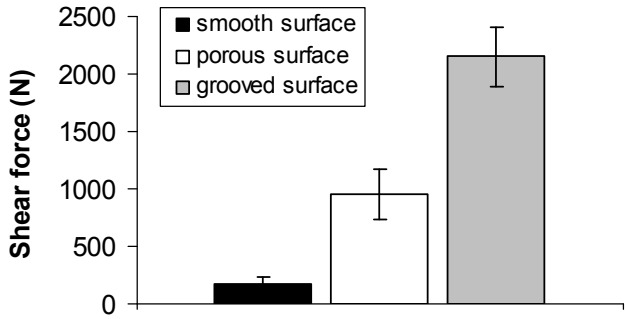

Figure 18. The results of the push-out force measurements in study II.

The Weibull analysis (Figure 5 in the original publication) showed higher reliability for the push-out force of FRC specimens with porous surface than for grooved implants, although their absolute and characteristic force values were lower.

There was mechanical strength in the porous interface of the implant after it was filled with dental stone, since the FRC implant did not break up into the porous and non-porous sections during the test. It can be hypothesized that in dynamic loading conditions, the porous surface layer containing short glass fibres could act as a stress breaking interface decreasing the stress-shielding. The push-out forces were over five times higher for surface porous FRC implants than for implants with smooth surface attaching only with friction. The push-out force of the implants with a grooved surface was higher than the cohesive strength of dental stone. This suggests that optimal implant design may contain a porous surface for microscopic bone attachment and grooves for macroscopic interlocking into bone.

Recently, animal models have been developed to study osseointegration of implants within load-bearing regions of trabecular bone. Materials were implanted into epiphyseal bone so that part of the compressive load in the knee went through the material (Frankenburg *et al.,* 1998; Ignatius *et al.,* 1997; Simon *et al.,* 2003). Healing of cancellous bone is more rapid than that of dense cortical bone due to large area of bone contacts in the defect area and rich blood supply to thin trabeculae (Salter, 1999). In study III, FRC with porous outermost surface were implanted in intercondular area of distal femur and the proximal tibia and push-out test was carried out in order to obtain information about fixation of the implant with the host bone. The results of the push-out test are presented in Figure 19. The push-out forces at the porous FRC-bone interface were statistically significantly higher than those at the solid PMMA-bone ($p < 0.001$) interface at all time intervals and Ti-bone ($p = 0.001$) interface at 12 weeks. The push-out force at 12 weeks post-operation at the bone-implant interfaces were 283.3, 14.4 and 130.6 N for FRC with porous surface, solid PMMA and solid Ti implants, respectively.

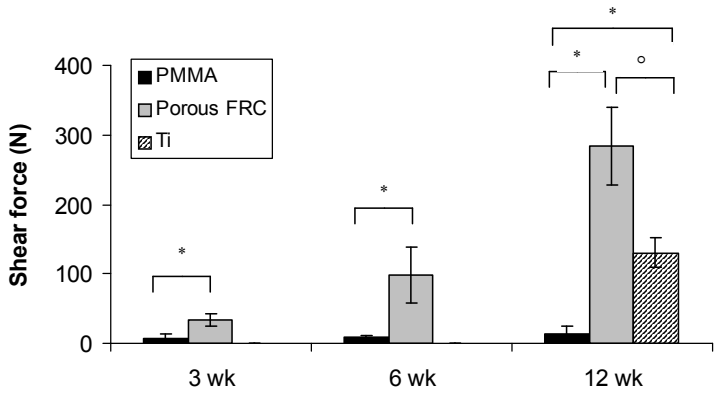

Figure 19. The results of push-out tests in study III. Ti implants were tested only at 12 weeks post-operation. Error bars represent standard deviations (n = 5-6). * and ° indicate a statistically significant difference ($p < 0.001$ and $p = 0.001$, respectively) between implant materials.

The animal experiment revealed that fixation between host bone and porous PMMA-based FRC implants had been achieved due to bone growth into the porous surface structure. In comparison, pure solid PMMA implants were surrounded by thick fibrous encapsulation.

6.3. Bone response

The surface chemistry and architecture of the implant are important parameters that influence protein absorption, cell interactions and host bone response. Densely packed, well-organised fibrous capsule is formed around non-porous implants while porous implants lead to a less dense and more disorganised fibrous capsule with increased vascularisation (Ratner and Bryant, 2004). The physiological response to surface porous implants is similar to the healing cascade of cancellous bone defects that occurs

principally through the formation of an internal or endosteal callus. External or periosteal callus surrounding cortex has also an important role in fracture healing (Salter, 1999).

6.3.1. Histological evaluation, histomorphometric and microradio-graphic analysis (III & IV)

Histological images of the animal experiments III and IV are presented in Figures 20 and 21, respectively. No inflammatory reactions were observed in histological evaluations.

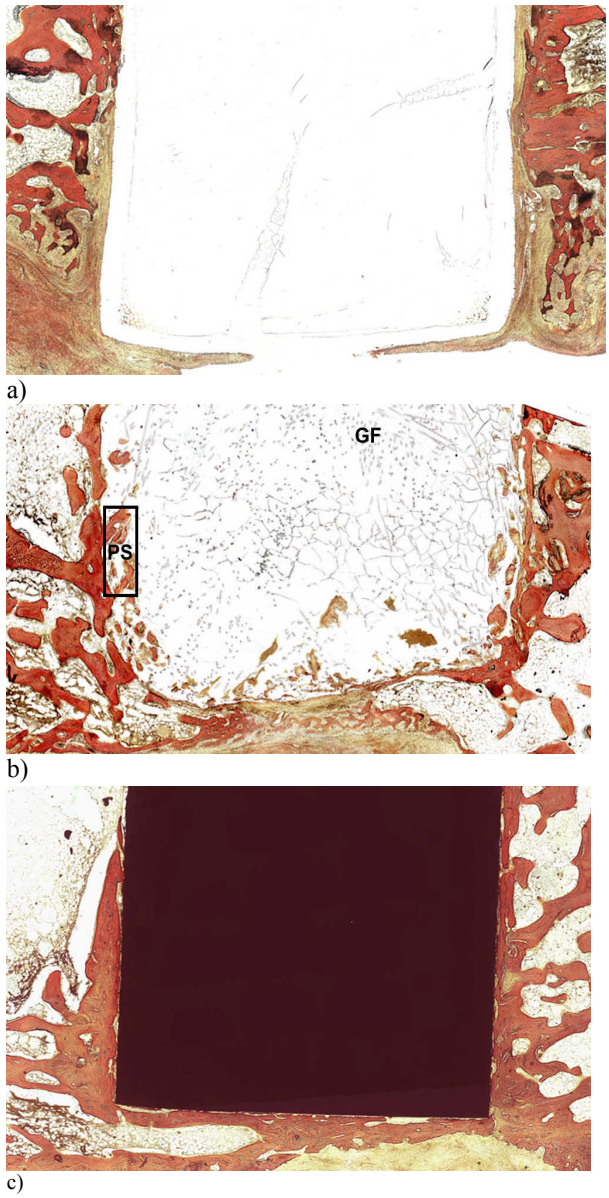

Figure 20. The histological images in study III. a) solid PMMA, b) FRC with a porous surface (PS = porous surface layer, GF = glass fibres) and c) solid Ti, all at 12 weeks post implantation. Van Gieson staining. Original magnification x5.

Study III

At 3 weeks, the histological evaluations revealed fibrous tissue growth into the pores of FRC implants. At 6 weeks, the pores were still mainly filled with connective tissue, but new bone formation inside porous structure was also observed. At 12 weeks (Fig. 20), new bone formation was evident, the FRC implants were well integrated into the host bone with irregular finger-like projections and the pores were filled with woven bone and connective tissue.

At 3 and 6 weeks, there were connective tissue encapsulations present around PMMA implants. At 12 weeks, a fibrous tissue layer was dominant at the interface of both PMMA and Ti implants, but some contacts with host bone and implants were also observed. In study III, fibrous tissue capsules were notably thicker ($p < 0.001$) around PMMA implants (241 ± 80 μm) than around Ti implants (79 ± 45 μm).

PMMA is susceptible to time-dependent deformation under constant loading, i.e. creep, which may lead to unstable bone-implant interface. In the case of FRC, viscoelastic yield point will be reached at higher stress level due to stress transfer from polymer matrix to glass fibres (Callister, 2007). The tendency for swelling during the surface porosity formation process led to slightly bigger diameter for FRC implants than for control PMMA implants and caused tighter press-fit insertion of FRC implants with porous surface. These factors, including also the difference in surface texturization, might have had an important effect on formation of fibrous capsule around PMMA implant.

Study IV

One of the rabbits in FRC group (20 wk) was abandoned because of incomplete operational alignment leading to false position of the implant. New bone formation was evident at 4 weeks as bridging trabeculous bone growing from the host periosteum junctions. Bone

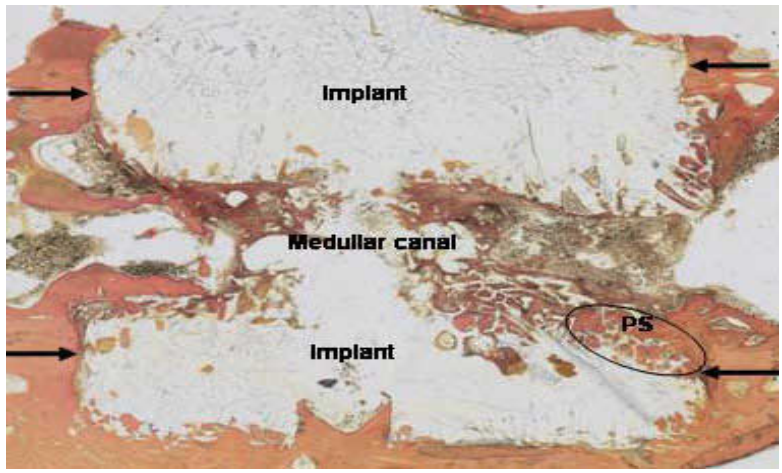

Figure 21. The histological image of FRC at 8 weeks post-operation, when new bone growth into porous surface structure of the implant was evident (PS = porous surface, cortical junctions pointed by arrows). Van Gieson staining. Original magnification x5. Study IV.

Table 5. Results of the histomorphometric analysis from segment defect study IV. Due to errors during the preparation of histological slides, BCI values at anterior and at the posterior surface of FRC implants at 20 weeks post-operation could not have been measured.

	n	Mean	Standard deviation	p-value
BCI at posterior surface (%)				
4 wk				
FRC	4	7.6	15.3	p = 0.850
Control	4	6.5	13.0	
8 wk				
FRC	5	27.0	30.5	p = 0.283
Control	4	10.7	21.4	
20 wk				
FRC	6	70.0	34.3	p = 0.050
Control	4	15.4	9.7	
BCI at anterior surface (%)				
4 wk				
FRC	4	1.9	3.8	p = 0.317
Control	4	0.0	0.0	
8 wk				
FRC	5	7.7	15.9	p = 0.850
Control	4	2.4	4.8	
20 wk				
FRC	0	N.A.	N.A.	N.A.
Control	4	3.3	5.6	
BCI at junctions (%)				
4 wk				
FRC	4	17.4	15.7	p = 0.561
Control	4	9.1	9.4	
8 wk				
FRC	5	53.9	50.5	P = 0.271
Control	4	16.1	21.3	
20 wk				
FRC	6	66.8	27.6	p = 0.034
Control	4	16.7	3.4	
BCI at intercortical area (%)				
4 wk				
FRC	4	45.6	39.7	p = 0.172
Control	4	12.5	25.0	
8 wk				
FRC	5	86.8	19.9	p = 0.375
Control	4	61.5	31.6	
20 wk				
FRC	6	96.3	6.8	p = 0.046
Control	4	45.6	38.3	
Total appositional bone growth at posterior site (area%)				
4 wk				
FRC	4	6.0	6.1	p = 0.714
Control	4	10.7	12.4	
8 wk				
FRC	5	55.3	29.0	p = 0.142
Control	4	23.4	24.2	
20 wk				
FRC	6	50.6	17.1	p = 1.000
Control	4	53.0	26.1	
Total appositional bone growth at anterior site (area%)				
4 wk				
FRC	4	0.8	1.6	p = 0.317
Control	4	0.0	0.0	
8 wk				
FRC	5	6.0	5.1	p = 0.282
Control	4	2.5	4.9	
20 wk				
FRC	0	N.A.	N.A.	N.A.
Control	4	14.9	6.6	
Intermedullary bone growth (area%)				
4 wk				
FRC	4	13.4	6.5	p = 0.014
Control	4	0.0	0.0	
8 wk				
FRC	5	7.5	5.8	p = 0.375
Control	4	4.4	5.0	
20 wk				
FRC	6	14.4	22.3	p = 0.825
Control	4	12.7	13.3	

growth into the medullar canal and into the pores of the FRC implant was also detected. Loose connective tissue was observed in some specimens near the interface of the dense core and porous surface layer of the FRC implant. At 8 weeks, new bone growth was more prominent in the case of the FRC implants with porous surface (Fig 21). A thick external trabeculous callus around the implant was formed especially at the posterior surface. At 20 weeks, lamellar bone was evident in all specimens and partially exposed E-glass fibres were embedded in lamellar bone. Due to bone remodelling process bone mass loss in the intermedullary canal was observed.

The results of histomorphometric evaluations are shown in Table 5. At 4 weeks, intramedullary bone growth was statistically significantly greater ($p = 0.014$) for FRC implants with porous surface than for PMMA control implants. At 20 weeks, the bone contact indexes (BCI) at the posterior side ($p = 0.050$), at the junction area ($p = 0.034$), and at the intercortical area ($p = 0.046$) showed significantly higher values for FRC implants with porous surface than in control implant group. At 20 weeks, BCI value and total appositional bone growth at anterior site were not able to be measured due to unsatisfactory quality of histological slides.

Figure 22 illustrates a microradiograph for FRC implant with porous surface at 8 weeks post-operation. The size of selected bioactive glass granules was not optimal and the distribution of granules was uneven. The appositional bone growth at the posterior site was more evident for porous FRC implant than for control group at 8 week. Strong bony callus over the posterior surface and trabecular bony bridge at intercortical area was detected at 8 weeks and it remodelled into lamellar bone by 20 weeks. There was no statistical difference between results gained by histomorphometrical and microradiographical methods as shown in figures 23a and 23b.

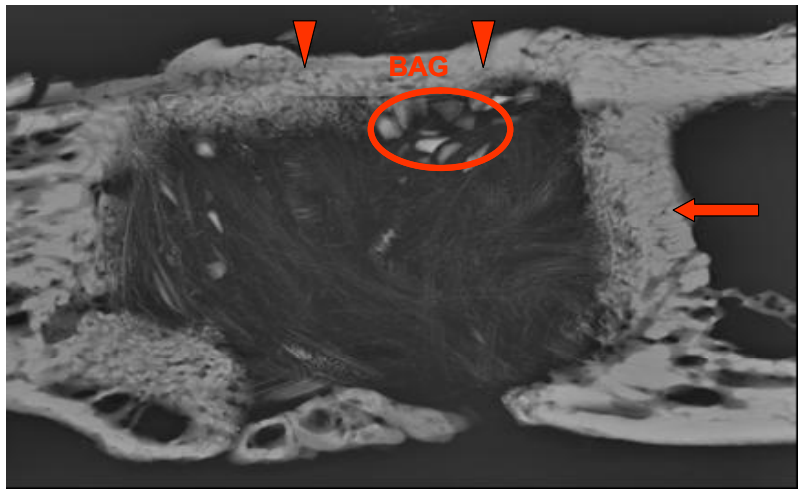

Figure 22. Microradiograph for FRC implant with porous surface at 8 weeks. Formation of bony bridge over the posterior surface (arrow heads) and at intercortical area (arrow). (BAG = bioactive glass granules Ø = 315-500 µm). Study IV.

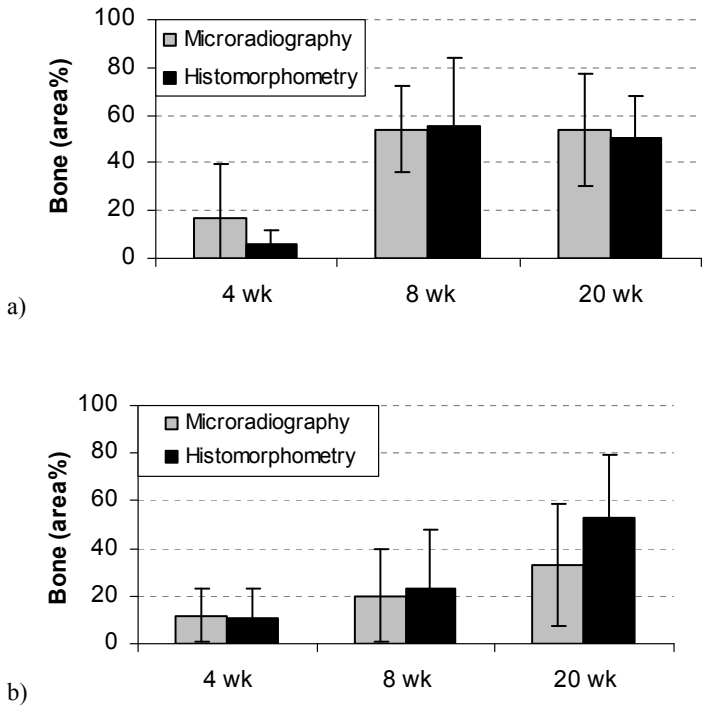

Figure 23. Comparion of histomorphometric and microradiographic analyses. a) FRC with porous surface and b) control PMMA implant with solid surface. No statistical difference was observed.

Histomorphometrical and microradiographical measurements in study IV revealed high values for total appositional bone growth on posterior site for both surface porous FRC (50.6 / 53.7 area%) and control PMMA (53.0 / 33.1 area%) implants at 20 weeks post-operation. Appositional bone growth values at posterior site were much higher compared to anterior site due to optimal blood supply from the surrounding muscles. Surface porous FRC implants showed significantly higher bone contact index values (BCI) than control implant group. According to another similar segment defect experiment, non-fibre-reinforced porous surface layer of PMMA may collapse partly during the implantation leading to a low BCI value (10 ± 8 %) at cortical junction area (Hautamäki *et al.,* 2008). In study IV, fibre-reinforced porous surface structure proved to have enough mechanical strength to tolerate compression during implantation in some extend, and these FRC implants revealed much higher BCI value (66.8 ± 27.6 %) at junction area.

To further enhance the fixation, surface-reactive osteoconductive bioactive glass particle or fibre inclusions can be embedded into polymer matrix of the composite. Bonding to bone is related to the simultaneous formation of calcium phosphate and SiO_2-rich layer on the surface of partly exposed bioactive additives (Billotte, 2007). In study IV, bioactive glass granules (S53P4) were included in composite structure and bonding contacts between granules and bone were observed. However, microradiographical evaluation revealed that neither size nor distribution of granules were optimal. Therefore, benefits

of bioactive glass additives were not fully exploited. Most probably, an even distribution of bioactive glass additives would have been obtained by replacing part of the E-glass fibres with bioactive glass fibres.

Both animal experiments in studies III and IV were performed in rabbits. The rabbit is one of the most commonly used animals for screening implant materials due to easy handling, convenient size and the fact that skeletal maturity is reached at the age of only 6 months. On the other hand, there are also drawbacks with the rabbit as an animal model. The size and the number of implants which may be inserted are limited. There are major differences in bone structure, composition, shape and loading between the rabbit and human. Bone remodelling process is also faster in rabbits than in humans. The performance of new implant material should be investigated in further *in vivo* studies in pigs which are considered to be closely representative of human bone (Pearce et al., 2007).

6.4. Finite element analysis

To ensure bone ingrowth, shear stresses and strains at the implant-bone interface should be minimized. In order to understand the mechanisms contributing to the higher interfacial strength found in the post *in vivo* push-out tests (study III) of FRC implants with a porous surface layer, finite element analysis was completed to find out the stress distribution that develops in different implant designs. FRC, PMMA and Ti implants with solid and porous surface layers were all analyzed.

6.4.1. Comparison of the shear stress distributions

The shear stress distributions for the cases simulating the push-out tests after 12 weeks healing are presented in Figure 24. For the solid PMMA and Ti implants the global model is presented, while for the FRC with porous surface the local model is plotted over the global model. The apparent shear strength was simply calculated from the force (66 N) divided by the area of the implant outer surface was 0.76 MPa. Values close to this are presented in orange in Figure 24. Only in the case of solid PMMA implant was this high shear stress acting on the implant-bone interface. The push-out force after 12 weeks of healing was less than 66 N for the PMMA implants, whereas it was significantly higher than 66N for both Ti and FRC implants. In the case of FRC with porous surface, the high shear stress was found from the implant material not from the pores. The model shows that the location of the shear stress peak value was different depending on if the implant had higher or lower Young's modulus (E) than the surrounding bone. For the FRC and Ti implants the highest shear stresses were found near the end of the supported edge, whereas for PMMA it was found near the loading surface. Both PMMA and FRC with porous surface transferred some shear stress to the surrounding bone whereas the Ti implant did not.

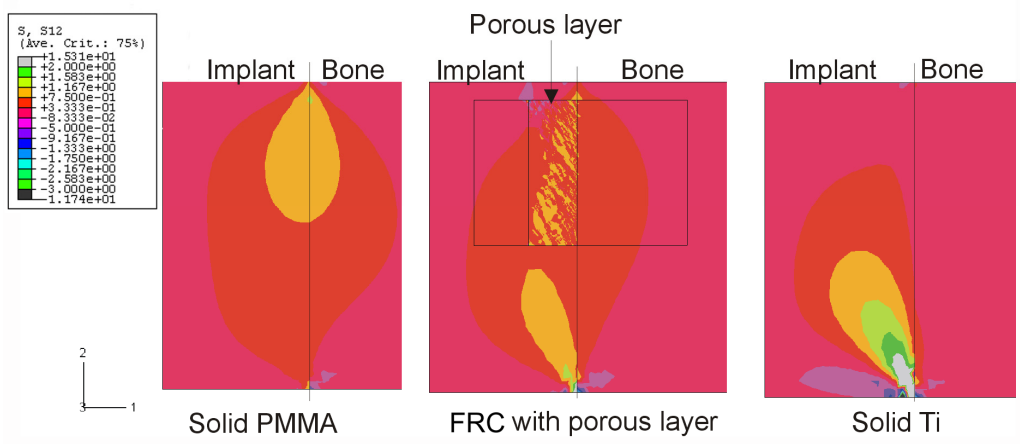

Figure 24. Shear stress distributions found in the cases that were tested post *in vivo* push-out after 12 weeks of healing. For the FRC with porous layer, the sub-model is plotted over the global model distribution. In all cases the push-out force was 66 N in direction –2 over total area of the implant, the lower edge of bone was fully supported. Study III.

All three implant materials were compared also as solid vs. porous layer, using the pore geometry of the FRC implant for all cases. With global model, it was not found any significant differences in the shear stress distributions. In global model, the porous layer had the effective elastic properties different from the core material. For the solid implant cases, the local model gave the same stress and strain distributions as the global model, which is exactly as it should be.

The local model revealed significant stress distributions for the cases of implants with porous layer (Fig. 25). For the PMMA implant with porous layer (lower E than that of the bone) the bone in the pores had higher shear stress than the implant material and than the bone surrounding the implant. According to the results of FEA, the FRC implants, with a porous surface layer, distributed the shear stress over the bone-implant interface more evenly than the porous PMMA and Ti implants did.

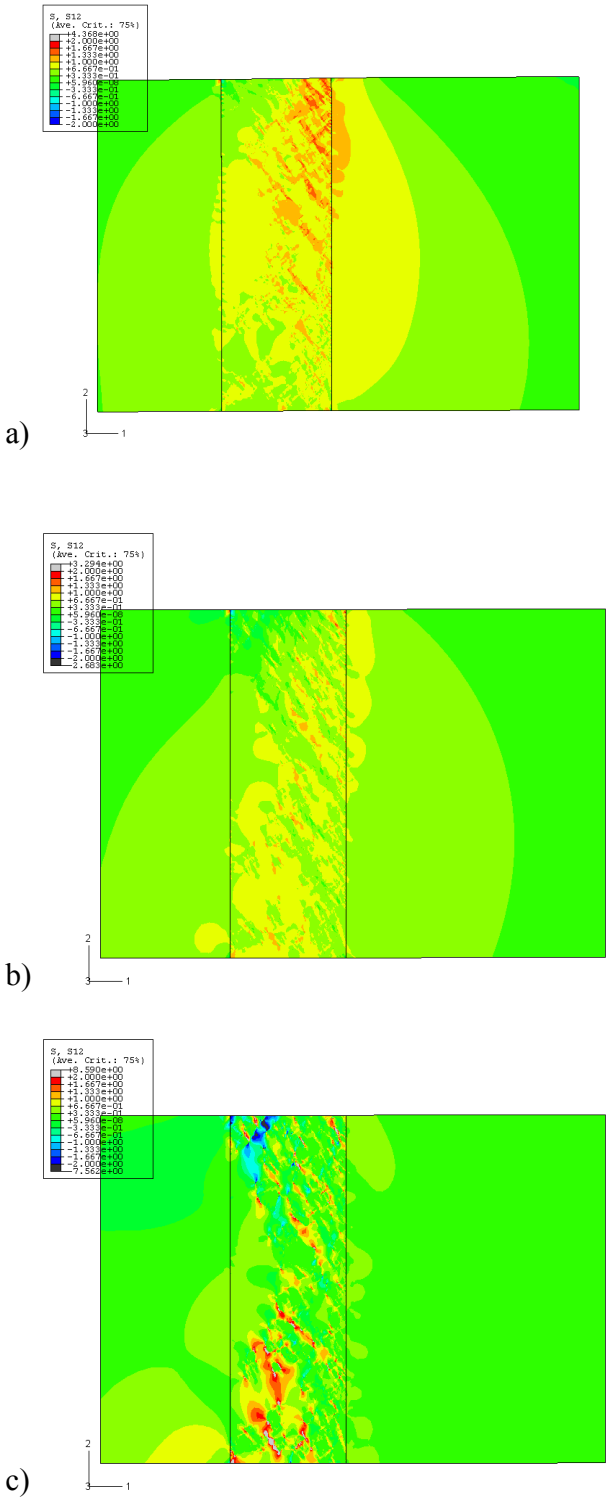

Figure 25. Shear stress distributions found in a) surface porous PMMA, b) surface porous FRC and c) surface porous Ti. Study III.

6.4.2. Comparison of the strain energy density (SED)

One issue to consider is the long-term properties of the attachment between porous layered implants and the bone. Overloading the bone at bone-pore interface leads to creep or fatigue, under-loading induces bone resorption and loosening of the implant. FEA was used to compare the strain energy densities of solid implants and implants with porous layers since the process is associated with the bone remodelling stimuli and is a measure of both the state of stress and strain. The SED values were more dependent on the elastic modulus of the implant material than on the porous surface structure. Figure 26 presents the strain energy density distributions (SED) of PMMA, FRC and Ti both as solid implant and with the porous layers.

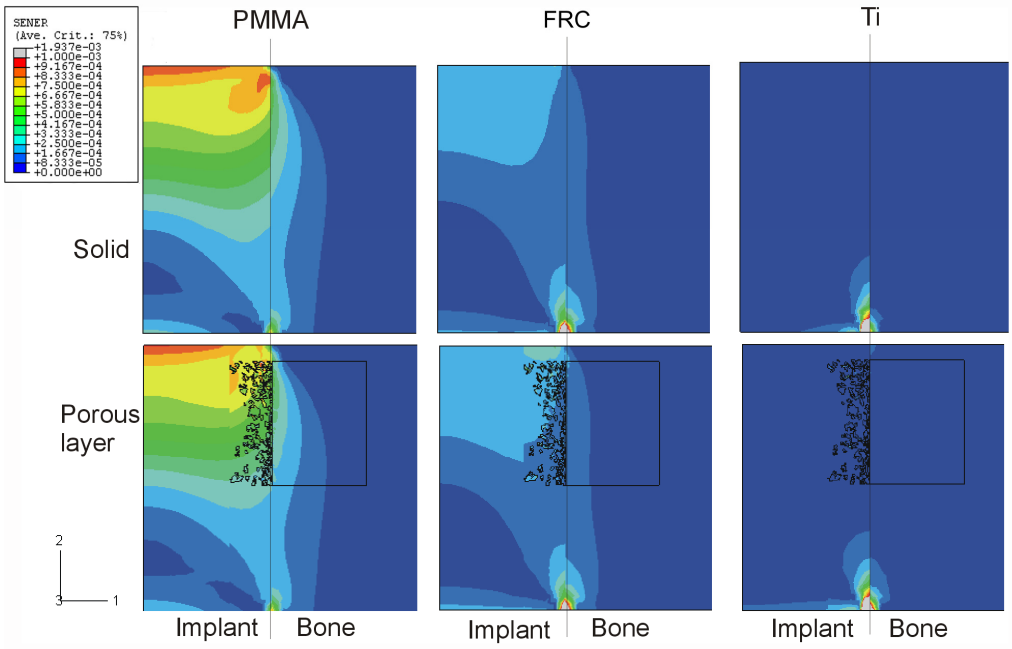

Figure 26. Strain energy density (mJ/mm^3) distributions in cases of solid implants (upper row) and implants with a porous layer (lower row). For the implants with a porous layer the sub-model showed only the areas of bone plotted over the global model. Study III.

The bone inside the pores and surrounding the implant faced more stress in the case of porous PMMA than it did with stiffer material such as porous FRC. The bone seemed to be clearly under-loaded if the implant material was the porous Ti. The presence of porous layer has very little effect on the SED-level of the bone surrounding the implant. The value of the Young's modulus of the implant was more dominant. It should be noted that the finite element model assumed tight fixation between implant and bone. However, the animal experiment indicated that FEA did not give realistic results in the case of PMMA implants. There was a thick fibrous encapsulation around solid PMMA implants and fixation between bone and implant did not occur.

6.5. General discussion and suggestions for future research

From the clinical perspective, study I was an attempt to develop a fibre-reinforced composite with a surface structure that allowed bone to grow into the material. Tetrahydrofuran (THF) solvent treatment was used in order to obtain swelling and dissolution of the PMMA on the surface of the specimen at room temperature. A porous surface was obtained by solidification of the swollen and dissolved PMMA layer and evaporation of the solvent THF. It was noticed that exposure of the randomly oriented short glass fibres played a significant role in porosity formation. Short fibres reinforced the porous surface and they may also prevent the collapse of the PMMA phase during porosity formation. The solvent residuals in the material, which can be diluted during the water storage period, need to be carefully investigated before proceeding with the testing protocol of biomaterial device development (study II).

In study II, mechanical interlocking and load-bearing capacity of FRC with porous surface was evaluated using dental stone as bone model material. It is likely that fibre-reinforced interconnective porous surface layer can withstand loading to the implant only when the pores are filled with bone. Animal experiments (III & IV) showed that new bone growth into the porous surface structure of FRC occurred and strong fixation between bone and implant was achieved. No adverse tissue reactions in the presence of partially exposed E-glass fibres were observed. Finite element analysis (FEA) revealed that FRC implants, with a porous surface layer, distributed the shear stress over the bone-implant interface more evenly than the porous PMMA and Ti implants did. Minimized shear stresses and strains at the bone-implant interface will ensure bone growth.

The available data on the biomechanical properties of the FRCs suggests that the strength and modulus of elasticity of the composite could be adequate for many biomaterial applications as presented in Table 6.

Table 6. Bending strength and elastic modulus of bone and some selected biomaterials ([#]Garbelini et al., 2003; [¤]Bouillaguet *et al.,* 2006; [+]Puska *et al*., 2004; *Yuehuei HA, 2000).

Material	Bending strength (MPa)	Elastic modulus in bending (GPa)
Ti-6Al-4V[#]	890	110
Unidirectional FRC (dry) [¤]	1150	26.2
Unidirectonal FRC (water storage) [¤]	759	25.5
Randomly orientated FRC (dry)[+]	130	8.1
Human cortical bone*	35 - 283	5 - 23

[¤]FRC included 42.3% of unidirectional E-glass fibres embedded in BisGMA-TEGDMA matrix; tested dry and after the water storage at 37°C for 1 month.

[+]FRC included 6% of chopped (l = 2 mm) E-glass fibres, 5% of ethylene glycol dimethacrylate (EGDMA) as a cross-linking monomer and Palacos®R (polymethylmethacrylate-polymethylacrylate) bone cement.

The strength and durability requirements for load-bearing implants are high. The effects of fatigue and physiological environment may reduce the strength of FRC implants greatly. For that reason, remarkable margin of safety for FRC implants is needed (Evans *et al*., 1998). Reinforcing effect of randomly orientated glass fibres may not be satisfactory for load-bearing endosseus implants. Optimisation of fibre volume, orientation and length is needed. FRC with a core made of unidirectional long fibres and a fibre-reinforced porous outermost layer might be an interesting option to be developed in the future. Torsional strength of the FRC could be increased with braided fabric. FEA provides a cheap and efficient tool to design novel FRCs intended to use as implants in various anatomical loading environments.

PMMA absorbs up to 2 % of water which can cause plasticization of the polymer matrix and degradation at the fibre-polymer matrix interface leading to decreased adhesion and stress transfer capacity (Cowperthwaite *et al*., 1981). The static strength of most composite materials gives only a small indication of their performance under prolonged cyclic loading. Long-term stability in aqueous environment, release of fibre debris and fatigue resistance of these FRC implants must be carefully studied in the future (Sundaresan *et al*., 1994). Giavaresi et al. have obtained promising mechanical and histomorphometric results with glass fibre-reinforced (35 v%) PMMA-based composites including hydroxyapatite granules (35 wt%) (Giavaresi *et al*., 2004). In further studies, part of the short E-glass fibres, which were exposed in the porous surface layer, could possibly be replaced with bioactive glass fibres to enhance the bone-bonding capability of porous FRC implant.

7. CONCLUSIONS

1. A method to fabricate FRCs with porous surface was developed. The exposure of the reinforcing fibres played a significant role in porosity formation. The thickness of the porous surface layer was dependent on the glass fibre quantity and solvent treatment time. The maximum pore size was 500 μm and interconnective porous structure was formed and was considered to be ideal for bone ingrowth.

2. Chopped glass fibre-reinforced porous surface layer was strong enough to carry load. The level of leachable residual monomer was considerably lower than those found in chemically cured fibre-reinforced dentures and in modified acrylic bone cements.

3. Porous FRC implant promoted fixation between bone and the implant. According to FE analysis, FRC implants with porous surface distributed the shear stress over the bone-implant interface more evenly the porous PMMA and Ti implants did.

4. New trabecular bone growth into the porous surface layer of FRC was observed at 8 weeks post-operation. At 20 weeks, lamellar bone was evident. Porous FRC implants showed significantly higher bone-implant contact index values compared to non-porous control implants. E-glass fibres did not cause any negative tissue response. Bone formation around E-glass fibres was detected at the bone-implant junctions.

The findings of the present study revealed that FRC with dense load-bearing core and porous surface structure could serve as an interesting alternative for metals in orthopaedics. However, more studies concerning mechanical characterisation, optimisation of reinforcement efficiency and fabrication techniques are needed.

ACKNOWLEDGEMENTS

This research work was carried out at the Department of Prosthetic Dentistry and Biomaterials Research, Institute of Dentistry, University of Turku, Finland, during the years 2002–2009. These studies were performed in part at the Bio- and Nanopolymers Research Group, Centre of Excellence at the Academy of Finland.

My warmest thanks go to Professor Pekka Vallittu for his encouraging guidance throughout these years and for giving me the opportunity to work in his group. I would like to express my gratitude to my other supervisor, Professor emeritus Allan Aho, for introducing me to the fascinating world of orthopaedic implants and sharing his knowledge of how to carry out *in vivo* experiments.

Thanks to Lippo Lassila for his expertise in statistical analysis and Mervi Puska for her patient guidance with HPLC analysis (and also for cleaning the column after my experiments!). I am very grateful to Pasi Alander for practical hands-on training with fabrication of fibre-reinforced composites in the lab.

Jami Rekola and Jarmo Gunn are warmly acknowledged for their work during the surgical part of the study. I would like to thank Päivi Mäki for preparation of histological slides and Jouko Sandholm from the Cell Imaging Core, Turku Centre for Biotechnology, for helping me with wide-field microscope. Dr. Erkki Svedström and Tarja Virsu from the Department of Diagnostic Radiology, University Central Hospital of Turku, are thanked for giving me a possibility to carry out microradiographical analysis.

The good co-operation with the co-authors Pirjo Laurila and Professor Tapio Mäntylä from Laboratory for Ceramic Materials, Department of Materials Science, Tampere University of Technology, are highly appreciated. It would not have been possible to include finite element analysis in this study without Pirjo's valuable contribution.

My sincere thanks go to all co-workers in FRC research group and personnel at the Institute of Dentistry for making the working atmosphere pleasant. Riitta Moberg and Tarja Peltoniemi are thanked for taking care of many practicalities. The personnel of Turku University Central Animal Laboratory are thanked for giving all the help needed with animals.

A special thanks goes to Madame Tuusa for absolutely the most hilarious and absurd moments during our congress trips to Cambridge, Barcelona and Faenza.

Thanks to the official pre-examiners of the thesis, Professor Reijo Lappalainen from the Department of Physics, University of Kuopio and Associate professor Rui Reis from the Department of Polymer Engineering, University of Minho, Portugal.

I would also like to thank Professor Jukka Seppälä from the Department of Biotechnology and Chemical Technology, Helsinki University of Technology for accepting the invitation

to function as my opponent at the public examination. Annika Karvonen is thanked for proofreading the language of the thesis.

I am grateful for the financial support from the National Technology Agency TEKES (Drug 2000 and Combio programmes) and Turku University Foundation.

Last but not least, I would like to thank you, Anne, Eiju, Hanna, Jasmina, Ketlin, Milla, Minttu and Sevi, for many unforgettable moments during and especially outside the office hours. I could not wish for nicer persons to work with!

Turku, August 2009

Riina Mattila

REFERENCES

Adam F, Hammer DS, Pfautsch S, Westermann K (2002) Early failure of a press-fit carbon fiber hip prosthesis with a smooth surface. J Arthoplasty 17: 217-223.

Akeson WH, Coutts RD, Woo SLY (1980) Principles of less rigid internal fixation with plates. Can J Surg 23: 235-239.

Akhavan S, Matthiesen MM, Schulte L, Penoyar T, Kraay MJ, Rimnac CM, Goldberg VM (2006) Clinical and histologic results related to a low-modulus composite total hip replacement stem. J Bone Joint Surg 88-A: 1308-1314.

Ali MS, French TA, Hastings GW, Rae T, Rushton N, Ross ER, Wynn-Jones CH (1990a) Carbon fibre composite bone plates. J Bone Joint Surg 72: 586-591.

Ali MS, French TA, Hastings GW, Rae T, Rushton N, Ross ERS, Wynn-Jones CH (1990b) Carbon fibre composite bone plates. Development, evaluation and early clinical experience. J Bone Joint Surg 72-B: 586-591.

Allcock S, Ali MA (1997) Case report: Early failure of a carbon-fiber composite femoral component. J Arthoplasty 12: 356-358.

Amis AA, Kempson SA, Camburn M, Radford WJ, Stead AC (1988) Anterior cruciate ligament replacement : biocompatibility and biomechanics of polyester and carbon fibre in rabbits. J Bone Joint Surg 74: 628-634.

Becker RO, Marino AA (1982) Chapter 4: Electrical Properties of Biological Tissue (Piezoelectricity). In: Electromagnetism & Life. Albany, New York: State University of New York Press.

Billotte WC (2007) Ceramic biomaterials. In: Biomaterials. Wong JY, Bronzino JD, editors. CRC Press, Boca Raton, FL, USA.

Bobyn JD, Pilliar RM, Cameron HU, Weatherly GC (1980) The optimum pore size for the fixation of porous-surfaced metal implants by the ingrowth of bone. Clin Orthop Rel Res 150: 263-270.

Bouillaguet S, Schutt A, Alander P, Schwaller P, Buerki G, Michler J, Cattani-Lorente M, Vallittu PK, Krejci I (2006) Hydrothermal and mechanical stresses degrade fiber-matrix interfacial bond strength in dental fiber-reinforced composites. J Biomed Mater Res B Appl Biomater 76: 98-105.

Bowen CR, Dent AC, Stevens R, Cain M, Steward M (2005) Determination of critical and minimum volume fraction for composite sensors and actuators. Proceedings 4M 2005 – First international conference on multi-material micro manufacture, Edited by Dimov S, and Menz W, Elsevier, 483-487.

Brekelmans WAM, Poort HW, Sloof TJJH (1972) A new method to analyses the mechanical behavior of skeletal parts. Acta Orthop Scand 43: 301-317.

Callister WD Jr (2007) Chapter 16 Composites. In: Materials Science and Engineering. An Introduction. 7th Edition. John Wiley & Sons Inc. York, PA, USA.

Chang, F., Pérez, J., Davidson, J.A (1990) Stiffness and strength tailoring of a hip prosthesis made of advanced composite materials. J Biomed Mater Res 24: 873-899.

Charnley J (1960) Anchorage of femoral head prosthesis to the shaft of the femur. J Bone Joint Surg 42-B: 28-30.

Cook SD, Thomas KA, Haddad RJ (1988) Histologic analysis of retrieved human porous-coated total joint components. Clin Orthop Rel Res 234: 90-101.

Cook SD, Barrack RL, Thomas KA, Haddad RJ (1989) Quantitative histologic analysis of tissue growth into porous total knee components. J Arthoplasty 4 (Suppl): 33-43.

Cowin SC (2001) Chapter 11.4 Shear properties of bone. In: Bone mechanics handbook. Second Edition. CRC Press, Boca Raton, FL, USA.

Cowperthwaite G, Foy JJ, Malloy MA (1981) Biomedical and dental applications of polymers. Gebelen CG and Koblitz FF, editors. Plenum, New York.

De Santis R, Ambrosio L, Nicolais L (2000) Polymer-based composite hip prostheses. J Inorg Biochem 79: 97-102.

De Santis R, Sarracino F, Mollica F, Netti PA, Ambrosio L, Nicolais L (2004) Continuous fibre reinforced polymers as connective tissue replacement. Comp Sci Tech 64: 861-871.

Dickinson BL (1989) UDEL polysulfone for medical applications. J Biomater Appl 3: 605-634.

Eschbach L (2000) Nonresorbable polymers in bone surgery. Injury Int J Care Injured 31: S–0 D22-27.

Evans SL, Gregson PJ (1998) Composite technology in load-bearing orthopaedic implants. Biomaterials 19: 1329-1342.

Frankenburg EP, Goldstein SA, Bauer TW, Harris SA, Poser RD (1998) Biomechanical and histological evaluation of a calcium phosphate cement. J Bone Joint Surg 80: 1112-1124.

Fujihara K, Teo K, Gopal R, Loh PL, Ganesh VK, Ramakrishna S, Foong KWC, Chew CL (2004a) Fibrous composite materials in dentistry and orthopaedics: review and applications. Comp Sci Tech 64: 775-788.

Fujihara K, Huang Z-M, Ramakrishna S, Satknanantham K, Hamada H (2004b) Feasibility of knitted carbon/PEEK composites for orthopaedic bone plates. Biomaterials 25: 3877-3885.

Galante JO, Sumner DR, Turner T, Barden R (1986) Fixation in total knee arthoplasty: fiber metal. In: Total Arthoplasty of the knee. Proceedings of the Knee Society 1985-1986. Edited by Rand JA, Dorr L. 236-248. Aspen Publishers, Rockville, USA.

Galante JO, Jacobs J (1992) Clinical performances of ingrowth surfaces. Clin Orthop Rel Res 276: 41-49.

Garbelini WJ, Henriques GEP, Troia M Jr, Mesquita MF, Dezan CC (2003) Evaluation of low-fusing ceramic systems combined with titanium grades II and V by bending test and scanning electron microscopy. Appl Oral Sci 11: 354-360.

Giavaresi G, Branda F, Causa F, Luciani G, Fini M, Nicoli Aldini N, Rimondini L, Ambrosio L, Giardino R (2004) Poly(2-hydroxyethyl methacrylate) biomimetic coating to improve osseointegration of a PMMA/HA/glass composite implant. *In vivo* mechanical and histomorphometric assessments. Int J Artificial Organs 27: 674-680.

Guo XE (2001) Mechanical properties of cortical bone and cancellous bone tissue. In: Bone Mechanics Handbook. Cowin SC, editor. CRC Press, Taylor & Francis Group, Boca Raton, FL, USA.

Hart RT (2001) Bone modelling and remodelling: theories and computation. In: Bone Mechanics Handbook. Cowin SC, editor. CRC Press, Taylor & Francis Group, Boca Raton, FL, USA.

Hautamäki MP, Aho AJ, Alander P, Rekola J, Gunn J, Strandberg N, Vallittu PK (2008) Repair of bone segment defects with surface porous fiber-reinforced polymethyl methacrylate (PMMA) composite prosthesis: Histomorphometric incorporation model and characterization by SEM. Acta Orthop 79: 555-564.

Heikkilä JT, Aho AJ, Kangasniemi I, Yli-Urpo A (1995) Polymethyl-methacrylate composites: disturbed bone formation at the surface of bioactive glass and hydroxyapatite. Biomaterials 17: 1755-1760.

Hench LL (1990) Bioactive glasses and glass-ceramics. In: CRC Handbook of Bioactive Ceramics. Yamamuro T, Hench LL, editors. CRC Press, Boca raton (FL), USA.

Hiermer T, Schmitt-Thomas KhG, Yang Z-G (1998) Mechanical properties and failure behaviour of cylindrical CFRP-implant-rods under torsion load. Composites 29A: 1453-1461.

Howard CB, Tayton KJ, and Gibbs A (1985) The response of human tissues to carbon reinforced epoxy resin. J Bone Joint Surg 67-B: 656-658.

Huiskes R, Nunamaker D (1984) Local stress and bone adaptation around orthopaedic implants. Calcified tissue International 36: S110-117.

Huiskes RH, Weinans H, Grootenboer J, Dalstra M, Fudala B, Slooff TJ (1987) Adaptive bone remodelling theory applied to prosthetic desing analysis. J Biomech 20: 1135-1150.

Huiskes R, Hollister SJ (1993) From structure to process, from organ to cell: recent developments of FE-analysis in orthopaedic biomechanics. J Biomed Eng 115: 520-527.

Huiskes R, Ruimerman R, van Lenthe GH, Janssen JD (2000) Effects of mechanical forces on maintenance and adaptation of form in trabecular bone. Nature 405: 704-706.

Hull D, Clyne TW (2002) An Introduction to Composite Materials: Cambridge University Press.

Ignatius A, Unterricker K, Wenger K, Richter M, Claes L, Lohse P, Hirst H (1997) A new composite made of polyurethane and glass ceramic in a loaded implant model: a biomechanical and histological analysis. J Mater Sci Mater in Med 8: 753-756.

Inoue K, Hayashi I (1982) Residual monomer (Bis-GMA) of composite resin. J Oral Rehabil 9: 493-497.

Jancar J, DiBenedetto AT (1993a) Fibre reinforced thermoplastic composites for dentistry. I. Hydrolytic stability of the interface. J Mater Sci Mater Med 4: 555-561.

Jancar J, DiBenedetto AT, Goldberg AJ (1993b) Thermoplastic fibre-reinforced composites for dentistry. II. Effect of moisture on flexural properties of unidirectional composites. J Mater Sci Mater Med 4:562-568.

Jasty M, Maloney WJ, Bragdon CR, O'Connor DO, T Haire, and WH Harris (1991) The initiation of failure in cemented femoral components of hip arthroplasties. J Bone Joint Surg 73-B: 551-558.

Jee WSS (2001) Intergated bone tissue physiology: anatomy and physiology. In: Bone Mechanics Handbook. Cowin SC, editor. CRC Press, Boca Raton, FL, USA.

Jenkins DHR (1978) The repair of cruciate ligaments with flexible carbon fibre: a longer term study of the induction of new ligaments and of the fate of the implanted carbon. J Bone Joint Surg 60-B: 520-522.

Jenkins DH, McKibbin B (1980) The role of flexible carbon-fibre implants as tendon and ligament substitutes in clinical practice. A preliminary report. J Bone Joint Surg 62-B: 497-499.

Katoozian H, Davy DT (2000) Effects of loading conditions and objective function on three-dimensional shape optimization of femoral components of hip endoprostheses. Med Eng Phys 22: 243-251.

Katoozian H, Davy DT, Arshi A, Saadati U (2001) Material optimization of femoral component of total hip prosthesis using fiber reinforced polymeric composites. Med Eng Phys 23: 503-509.

Kruger T, Alter C, Reichel H, Birke A, Hein W, Spielmann RP (1998) Possibilities of follow-up imaging after implantation of a carbon fiber-reinforced hip prosthesis. Aktuelle Radiol 8: 81-86.

Latour RA, Black J (1993) Development of FRP composite structural biomaterials: fatigue strength of the fiber/matrix interfacial bond in simulated *in vivo* environments. J Biomed Mater Res 27: 1281-1291.

Lewandowska-Szumie LM, Komender J, Gorecki A, Kowalski M (1997) Fixation of carbon fibre-reinforced carbon composite implanted into bone. J Mater Sci Mater Med 8: 485-488.

Linder L, Hansson HA (1983) Ultrastructural aspects of the interface between bone and cement in man. Report of three cases. J Bone Joint Surg 65-B: 646-649.

Lynch CT (1989) Practical Handbook of Materials Science. CRC Press, Boca Raton, FL, USA.

Mano JF, Sousa RA, Boesel LF, Neves NM, Reis RL (2004) Bioinert, biodegradable and injectable polymeric matrix composites for hard tissue replacement: state of the art and recent developments. *Comp Sci Tech* 64: 789-817.

Marcolongo M, Ducheyne P, Garino J, Schepers E (1998) Bioactive glass fiber/polymeric composites bond to bone tissue. J Biomed Mater Res 39: 161-170.

McKenna GB, Bradley GW, Dunn HK, Statton WO (1980) Mechanical properties of some fibre reinforced polymer composites after implantation as fracture fixation plates. Biomaterials 1: 189-192.

Merolli A, Perrone V, Tranquilli Leali P, Ambrosio L, De Santis R, Nicolais L, Gabbi C (1999) Response to polyetherimide based composite materials implanted in muscle and in bone. J Mater Sci Mater Med 10: 265-268.

Miettinen VM, Vallittu PK (1997) Release of residual methyl methacrylate into water from glass fibre-poly(methyl methacrylate) composite used in dentistry. Biomater 18: 181-185.

Morrison C, Macnair R, MacDonald C, Wykman A, Goldie I, Grant MH (1995) *In vitro* biocompatibility testing of polymers for orthopaedic implants using cultured fibroblasts and osteoblasts. Biomaterials 16: 987-992.

Murphy J (1998a) Design Data. In: Reinforced Plastics Handbook. Oxford: Elsevier Science Ltd, 251-293.

Murphy J (1998b) Reinforcements. In: Reinforced Plastics Handbook. Oxford: Elsevier Science Ltd, 63-106.

Mäkisalo SE, Paavolainen PP, Lehto M, Skutnabb K, Slatis P (1989) Collagen types I and III and fibronectin in healing anterior cruciate ligamnet after reconstruction with carbon fibre. Injury 20: 72-76.

Olea N, Pulgar R, Pérez P, Olea-Serrano F, Rivas A, Novillo-Fertrell A, Pedraza V, Soto AM, Sonnenschein C (1996) Estrogenicity of resin-based composites and sealants used in dentistry. Evinron Health Perspect 104: 298-305.

Padmanabhan K, Kishore A (1995) Failure behaviour of carbon fibre/epoxy composites in pin-ended buckling and bending tests. Composites 26: 201-206.

Park JB, Lakes RS (2007) Electrical properties of bone. In: Biomaterials: An Introduction. Springer.

Park SH, Llinás A, Goel VK, Keller JC (2007) Chapter 9.1.2.1. Implant fixation method, In: Biomaterials. Wong JY, Bronzino JD, editors. CRC Press, Taylor & Francis Group, Boca Raton, FL, USA.

Pearce AI, Richards RG, Milz S, Schneider E, Pearce SG (2007) Animal models for implant biomaterial research in bone: a review. European Cell and Materials 13: 1-10.

Peluso G, Petillo O, Ambrosio L, Nicolais L (1994) Polyetherimide as biomaterial: preliminary *in vitro* and *in vivo* biocompatibility testing. J Mater Sci Mater Med 4: 738-742.

Pemberton DJ, McKibbin B, Savage R, Tayton K, Stuart D (1992) Carbon-fibre reinforced plates for problem fractures. J Bone Joint Surg 74-B: 88-92.

Peutzfeltdt A, Sahafi A, Asmussen E (2000) Characterization of resin composites polymerized with plasma arc curing units. Dent Mater 16: 330-336.

Pirhonen E (2006) PhD thesis: Fibres and composites for potential biomaterials applications. Tampere University of Technology, publication 599. Tampere, Finland.

Puska MA, Närhi TO, Aho AJ, Yli-Urpo A, Vallittu PK (2004) Flexural properties of crosslinked and oligomer-modified glass-fibre reinforced acrylic bone cement. J Mater Sci: Mater Med 15: 1037-1043.

Ramakrishna S, Mayer J, Wintermantel E, Leong KW (2001) Biomedical applications of polymer-composite materials: a review. Comp Sci Tech 61: 1189-1224.

Ratner BD, Bryant SJ (2004) Biomaterials: Where we have been and where we are going. Annu Rev Biomed Eng 6: 41-75.

Rohner B, Wieling R, Magerl F, Schneider E, Steiner A (2005) Performance of a composite flow moulded carbon fibre reinforced osteosynthesis plate. Vet Comp Orthop Traumatol 18: 175-82.

Rubin CT, Lanyon LE (1985) Regulation of bone mass by mechanical strain magnitude. Calcified Tissue International 37: 411–417.

Rushton N, Dandy DJ, Naylor CP (1983) The clinical, arthroscopic and histological findings after replacement of the anterior cruciate ligament with carbon fibre. J Bone Joint Surg 65-B: 308-309.

Sakaguchi M, Nakai A, Hamada H, Takeda N (2000) The mechanical properties of unidirectional thermoplastic composites manufactured by a micro-braiding technique. Comp Sci Tech 60: 717-722.

Salame K, Ouaknine GER, Razon N, Rochkind S (2001) The use of carbon fiber cages in anterior cervical interbody fusion. Report of 100 cases. Neurosurg Focus 12: 1-5.

Salter RB (1999) Musculoskeletar Injuries. In: Textbook of disorders and injuries of the musculoskeletal system: an introduction to orthopaedics, fractures, and joint injuries, rheumatology, metabolic bone disease, and rehabilitation. Lippincott Williams & Wilkins.

Santerre JP, Shajii L, Leung BW (2001) Relation of dental composite formulations to their degradation and the release of hydrolyzed polymeric-resin-derived products. Crit Rev Oral Biol Med 12: 136-151.

Sarkar BK (1998) Estimation of composite strength by a modified rule of mixtures incorporating defects. Bull Mater Sci 21: 329-333.

Schils F, Rilliet B, Payer M (2006) Implantation of an empty carbon fiber cage or a tricortical iliac crest autograft after cervical discectomy for singlelevel disc herniation: a prospective comparative study. Spine 4: 292–299.

Schmitt-Thomas KhG, Zhen-Guo Y, Hiermer T (1998) Development of torsion loading facility used for evaluating shear performance of polymeric composite implant rods. Polymer testing 17: 117-130.

Simon U, Augat P, Ignatius A, Claes L (2003) Influence of the stiffness of bone defect implants on the mechanical conditions at the interface – a finite element analysis with contact. J Biomech 36: 1079-1086.

Søballe K, Hansen ES, Brockstedt-Rasmussen H, Pedersen CM, Bünger C (1990) Hydroxyapatite coating enhances fixation of porous coated implants. A comparison in dogs between press fit and noninterference fit. 61: 299-306.

Søballe K, Hansen ES, Rassmussen HB, Jorgensen PH, Bunger C (1992) Tissue ingrowth into titanium and hydroxyapatite-coated implants during stable and unstable mechanical conditions. J Orthop Res 10: 285-299.

Spealman CR, Main RJ, Haag HB, Larson PS (1945) Monomeric methyl methacrylate. Studies on toxicity. Industrial Medicine 14: 292-298.

Sundaresan MJ, Henneke EG, Reifsnider KL (1994) Prediction of fatigue life of composite femoral prostheses using acoustic-emission technique. J Comput Tech Res 16: 127-131.

Sundfeldt M, Carlsson LV, Johansson CB, Thomsen P, Gretzer C (2006) Aseptic loosening, not only a question of wear: A review of different theories. Acta Orthopaedica 77: 177 – 197.

Szmukler-Moncler S, Salama H, Reingewirtz Y, Dubruille (1998) Timing of loading and effect of micromotion on bone-dental implant interface: Review of experimental literature. J Biomed Mater Res (Appl Biomater) 43: 192-203.

Tanimoto Y, Nishiwaki T, Nemoto K (2004) Numerical failure analysis of glass-fiber-reinforced composites. J Biomed Mater Res 68A: 107-113.

Taylor M, Tanner KE, Freeman MAR, Yettram AL (1995) Finite element modelling – predictor of implant survival? J Mater Sci Mater Med 6: 808-812.

Tuusa S (2007) PhD thesis: Development of craniofacial bone defect reconstruction implant based on fibre-reinforced composite with photopolymerisable resin system: Experimental studies *in vitro* and *in vivo*. Annales Universitatis Turkuensis. Ser D, Tom 771. Turku, Finland.

Vallittu PK. (1996) A review of fiber-reinforced denture base resins. J Prosthod 5: 270-276.

Vallittu PK (1997) Oxygen inhibition of autopolymerization of polymethyl-methacrylate-glass fiber composite. J Mater Sci Mater Med 8: 489-492.

Vallittu PK, Ekstrand K (*1999) In vitro* cytotoxicity of fibre-polymethyl methacrylate composite used in dentures. J Oral Rehabil *26*: *666*-671.

Vallittu PK (2001) Strength and interfacial adhesion of FRC-tooth system. In: The Second International Symposium on Fibre-reinforced Plastics in Dentistry, 13 October 2001, Nijmegen, The Netherlands. Vallittu PK, editor. Turku, Finland and Nijmegen, The Netherlands.

van Loon JJ, Bierkens J, Maes J, Schoeters GE, Ooms D, Doulabi BZ, Veldhuijzen JP (1995) Polysulphone inhibits final differentiation steps of osteogenesis *in vitro*. *J* Biomed Mater Res 29: 1155-1163.

Wan YZ, Chen GC, Huang Y, Li QY, Zhou FG, Xin JY, Wang YL (2005) Characterization of three-dimensional braided carbon/Kevlar hybrid composites for orthopedic usage. Mater Sci Eng A398: 227–232.

Veerabagu S, Fujihara K, Dasari GR, Ramakrishna S (2003) Strain distribution analysis of braided composite bone plates. Comp Sci Tech 62: 427-435.

Venhoven BAM, de Gee AJ, Werner A, Davidson CL (1994) Silane-treatment of filler and composite blending in a one-step procedure for dental restoratives. Biomaterials 15: 1152-1156.

Wenz LM, Merritt K, Brown SA Moet A (1990) *In vitro* biocompatibility of polyetherketone and polysulfone composites. J Biomed Mater Res 24: 207–215.

Väkiparta M, Koskinen MK, Vallittu P, Närhi T, Yli-Urpo A (2004) *In vitro* cytotoxicity of E-glass fiber weave preimpregnated with novel biopolymer. J Mater Sci Mater Med 15: 69-72.

Williams A, McNamara R (1987) Potential of polyetheretherketone and carbon fiber-reinforced PEEK in medical applications. J Mater Sci Lett 6: 188-190.

Williams DF (1999) The Williams dictionary of biomaterials. Liverpool University Press, Liverpool, UK.

Wolff J (1986) The law of bone remodelling. Translated by Maquet PGJ and Furlong R. Springer-Verlag, New York, USA.

Yildiz H, Chang F-K, Goodman S (1998) Composite hip prosthesis design. II Simulation. J Biomed Mater Res 39: 102-119.

Yuehuei HA (2000) Mechanical properties of bone. In: Mechanical Testing of Bone and the Bone-Implant Interface. Yuehuei HA and Draughn RA, editors. CRC Press LLC, Boca Raton, FL, USA.

Zhang G, Latour RA, Kennedy JM, Del Schutte H, Friedman RJ (1996) Long-term compressive property durability of carbon fibre-reinforced polyetheretherketone composite in physiological saline. Biomaterials 17: 781-789.

Zhao DS, Moritz N, Laurila P, Mattila R, Lassila LV, Strandberg N, Mäntylä T, Vallittu PK, Aro HT (2008) Development of a multi-component fiber-reinforced composite implant for load-sharing conditions. Med Eng Phys 31: 461-469.